

Solar Thermochemical Hydrogen Production Research (STCH)

Thermochemical Cycle Selection and Investment Priority

Submitted by Robert Perret in accord with contract

January 12, 2011

Executive Summary

Eight cycles in a coordinated set of projects for Solar Thermochemical Cycles for Hydrogen production (STCH) were evaluated on October 8 and 9, 2008. This document reports the initial selection process for development investment in STCH projects, the evaluation process meant to reduce the number of projects as a means to focus resources on development of a few most-likely-to-succeed efforts, the obstacles encountered in project inventory reduction and the outcomes of the evaluation process. Summary technical status of the projects under evaluation is reported and recommendations made to improve future project planning and selection activities.

The initial selection process reduced more than 350 possible cycles to 14 cycles in 5 reaction classes. Of these 14 cycles, 2 were under separate funding and management authority, 3 were quickly abandoned after preliminary laboratory study showed them to be unworkable and another 3 were never engaged actively because of obvious disadvantages. The remaining 6 cycles were actively pursued (2 under the Office of Nuclear Energy) and a fifth cycle was added later by the Office of Energy Efficiency and Renewable Energy. New discoveries and alternative reaction paths added 2 more cycles so that the October 2008 evaluation considered 9 thermochemical reaction cycles.

None of the cycles under evaluation could demonstrate substantively that they would meet published performance targets. Performance targets were under revision at the time of the evaluation and a compelling case to terminate efforts for lack of performance was not made. Not all cycles adhered faithfully to the mandated analysis framework and so comparative assessment of reported performance or potential performance was not possible from the evaluation. Finally, cycle development maturity was widely disparate, with periods of study ranging from less than a year to more than 30 years. Consequently, an equitable framework for comparative assessment of achievement was impossible and comparisons would necessarily be based on a mix of achievement and projected performance. Finally, nearly all cycles under development reported single-point failure challenges whose successful prosecution would be necessary for the cycle to promise competitive performance.

Decision-making for focused resource investment turned away from cycle termination to focused investment in resolution of those critical path obstacles to competitive potential. Critical path challenges for each cycle are identified that teams have been directed to pursue with top priority to assist in resource investment decisions in the near future.

Summaries of project status and the evaluation process led to recommendations for early involvement of external experts in project planning activities to help focus investments from the outset on critical process elements essential to successful project completion. Additional recommendation is made for continuing review and re-planning of project priorities as more information is developed. Finally, recommendation is made for the appointment of an external body of experts to implement a process for termination or continuation decisions.

Table of Contents

1. Introduction	1
2. Cycle Inventory Development and Selection Process	5
3. Formal Cycle Evaluation and Research Prioritization	16
4. Cycle Status Summaries and Path Forward Recommendations	29
4.1 Sulfur Iodine	29
4.2 Hybrid Sulfur	35
4.3 Photolytic Sulfur Ammonia	40
4.4 Zinc Oxide	44
4.5 Cadmium Oxide	48
4.6 Sodium Manganese Cycle	55
4.7 Sodium Manganate	60
4.8 ALD Ferrite	61
4.9 Hybrid Copper Chloride	64
5. Summary	68
5.1 General Observations	68
5.2 Evaluation Outcomes	
5.2.1 Sulfur Iodine	69
5.2.2 Hybrid Sulfur	70
5.2.3 Photolytic Sulfur Ammonia	70
5.2.4 Zinc Oxide	70
5.2.5 Cadmium Oxide	71
5.2.6 Sodium Manganese	71
5.2.7 Sodium Manganate	72
5.2.8 ALD Ferrite	73
5.2.9 Hybrid Copper Chloride	73
5.3 Recommendations	
5.3.1 Project planning	74
5.3.2 Selection process	75
Reference Materials	76

List of Figures

Fig. 1.1 Thermochemical cycle class examples

Figure 4.1.1 Sulfur Iodine three-step cycle

Figure 4.1.1 Bayonet decomposition reactor designed by Sandia National Laboratories

Figure 4.1.2 Bayonet decomposition reactor manifold designed by Sandia National Laboratories

Figure 4.1.3 Schematic solar interface with the solid particle receiver with intermediate heat exchanger providing heated He gas to drive the decomposition reactor

Figure 4.1.4 Bunsen reaction flowsheet (section 1)

Figure 4.1.5 Acid decomposition flowsheet (section 2)

Figure 4.1.6 HI decomposition flow sheet (section 3)

Figure 4.2.1 The Hybrid Sulfur cycle

Figure 4.2.2 Schematic of PEM membrane in the Hy-Sulfur electrolysis step

Figure 4.2.3 Hybrid Sulfur flowsheet

Figure 4.2.4 H2A hydrogen cost estimates for Hybrid Sulfur

Figure 4.3.1. Photolytic Sulfur Ammonia schematic process

Figure 4.3.2 Process chemistry for Photolytic Sulfur Ammonia

Figure 4.3.3 AspenPlusTM flow sheet for Sulfur Ammonia cycle

Figure 4.4.1 Zinc Oxide cycle chemistry

Figure 4.4.2 Zinc Oxide cycle flowsheet (CU Final Report)

Figure 4.4.3 ZnO plant cost allocation for the 2015 case study

Figure 4.4.4 ZnO plant cost allocation for the 2025 case study

Figure 4.5.1 Chemical steps of the Cadmium Oxide cycle

Figure 4.5.2 Process flow for a diurnal solar cadmium oxide hydrogen cycle

Figure 4.5.3 Conceptual rotating kiln counter flow hydrolysis reactor with tungsten carbide balls to enhance steam/Cd interaction

Figure 4.5.4 Beam down collector integrated with fluidized bed decomposition receiver/reactor

Figure 4.5.5 CdO cycle flowsheet, AIChE Meeting, Salt Lake City, November 7, 2007

Figure 4.6.1 Schematic steps for the Sodium Manganese cycle

Figure 4.6.2 Mixed metal oxide steps for the Sodium Manganese cycle

Figure 4.6.3 Schematic flowsheet for analysis of the Mx-Sodium Manganese cycle

Figure 4.6.4 System layout with a single chemical plant for the Mx-Sodium Manganese cycle

Figure 4.6.5 Estimated capital cost distribution for the mixed metal oxide realization of the Sodium Manganese cycle

Figure 4.7.1 Reaction path for the preliminary Sodium Manganate cycle

Figure 4.8.1 Schematic chemistry of a water-splitting ferrite cycle

Figure 4.8.2 ALD deposition of uniform thin layer of cobalt ferrite

Figure 4.9.1 Hybrid Copper Chloride chemistry

Figure 4.9.2 Hy-CuCl conceptual block flow chart

List of Tables

Table 1.1 DOE Performance Targets
Table 2.1 Relative importance of criteria to plant development and operation
Table 2.2 Solar-device criteria weighting factors
Table 2.3 Criteria scoring scheme
Table 2.4 Listing of non-zero efficiencies for top-scoring cycles
Table 2.5 Cycles that could move to Phase 3 detailed theoretical and experimental study
Table 3.1 Cycles considered in the formal evaluation process
Table 3.2 Cycle feasibility assessments
Table 3.3 Conceptual system design issues
Table 3.4 DOE performance targets issues
Table 3.5 Summary of evaluation outcomes
Table 4.1.1 Sulfur-Iodine cycle advantages and challenges
Table 4.2.1 Hybrid Sulfur advantages and challenges
Table 4.3.1 Advantages and challenges for Photolytic Sulfur Ammonia
Table 4.4.1 Advantages and challenges for Zinc Oxide
Table 4.5.1 Advantages and challenges for the Cadmium Oxide cycle
Table 4.5.2 Component capital costs cited for CdO cycle at the time of the evaluation
Table 4.5.3 CdO operating costs cited at the time of the evaluation
Table 4.5.4 Assumptions for 2015 case study cost analysis
Table 4.5.5 CdO cost estimates with some sensitivity estimates
Table 4.6.1 Advantages and challenges for Mx-Sodium Manganese
Table 4.6.2 Component uncertainties for the Mx-Sodium Manganese cycle
Table 4.9.1 Advantages and challenges for Hy-CuCl
Table 4.9.2 Hy-CuCl system performance sensitivity to electrolyzer performance
Table 4.9.3 H2A analysis results for Hy-CuCl

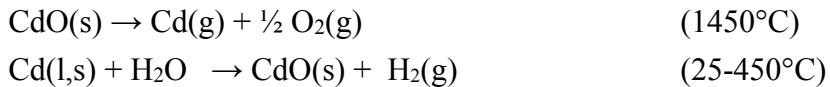
1. Introduction

STCH Basis:

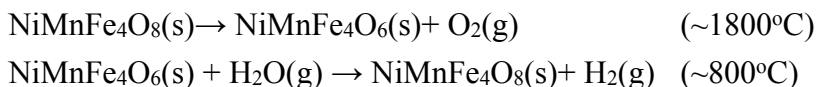
The Solar Thermochemical Hydrogen Production (STCH) project focuses on solar-powered thermochemical water splitting to produce hydrogen using water and solar thermal energy as the only feedstocks. Thermochemical hydrogen production has been under study at one level or another for many years. Most recently, renewable sources of thermal energy, like solar and nuclear reactor sources, have been emphasized. Nuclear power represents a high energy density source that is restricted in operating temperature range because of the materials of construction needed to contain nuclear material. Solar power represents a low energy density source that can attain far higher temperatures through solar concentration, but is still restricted in operating temperature because of materials of construction needed to contain the thermochemical reaction. Nevertheless, feasible operating temperatures for a solar cycle are much higher than those for a nuclear cycle. As a consequence, the inventory of possible solar-powered thermochemical reactions to produce hydrogen from water is quite large.

A simple two-step thermochemical water-splitting reaction to produce hydrogen generally requires very high temperature heat for endothermic metal oxide reduction to release oxygen, and a lower temperature exothermic reaction of water with the metal, increasing the oxidation state of the metal and releasing hydrogen. In most two-step cycles of this sort, the reduction temperature exceeds the vaporization temperature of the metal and this class is called the Volatile Metal Oxide class. Several two-step metal oxide cycles have been investigated in which mixed oxides, usually ferrite compounds, undergo reduction and oxidation without volatilization and these and other non-volatile multi-step reactions were assigned to a Non-Volatile Metal Oxide class. All of the reactions in these two classes rely on very high temperatures ($>1400^{\circ}\text{C}$).

Thermal reduction of some more complex chemicals can be achieved at lower temperatures because the oxygen bonds are weaker than for simple metal oxides. An intermediate reaction is necessary to release hydrogen and another reaction (sometimes more than one) is required to restore the oxidation state of the initial compound. Most lower temperature cycles either employ intermediates for oxidation, complicating the cycle chemistry, or use electrolysis to release hydrogen and restore the original oxidation state of the cycle. A sulfuric acid cycle is one of very few low temperature pure thermochemical cycles that operate at moderately high temperature ($\sim 850^{\circ}\text{C}$), but it is a multi-step cycle with an intermediate compound required to close the cycle. Another sulfuric acid cycle is simplified to a two-step cycle by using an electrolytic step to close the cycle. Electrolytic cycles are assigned to a Hybrid Reaction class.

Volatile Metal Oxide:**Non-Volatile Metal Oxide:**

Ferrite:



Multi-step cycle:

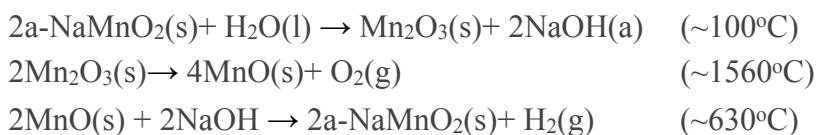
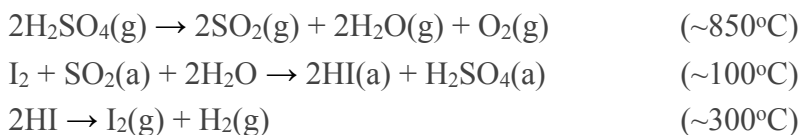
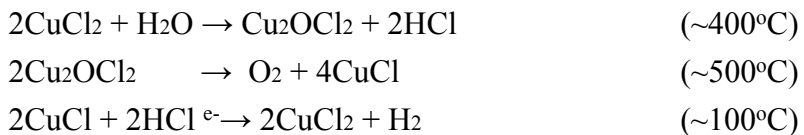
**Sulfuric Acid:****Hybrid Copper Chloride:**

Fig. 1.1 Thermochemical cycle class examples

Examples of these reaction classes from the inventory of thermochemical cycles that were actively studied under STCH are shown above (Fig. 1.1). The Sulfuric Acid class was studied primarily under the auspices of the Office of Nuclear Energy, but these are included since STCH supported integration of this class with a solar power interface in lieu of a nuclear power interface.

STCH Decision Framework:

The STCH project was founded as an applied research and development effort to identify the most promising cycle or cycles and develop a pilot plant design (or designs) for construction, operation and evaluation. The effort was organized into three investigative phases. It was known from the outset that there are many closed thermochemical cycles capable of splitting water and releasing hydrogen, so the Phase 1 objective was to document the known candidate

cycles (>350) and then select a smaller number (~50) of promising candidates for somewhat more detailed investigation. Phase 2 applied HSC Chemistry modeling to establish reaction temperatures necessary for completion of each cycle step and simplified flow charts for the chemical process were developed to estimate the cycle thermodynamic efficiency. A base line efficiency was chosen and cycles with efficiencies exceeding the baseline were selected to move into Phase 3. Quantitative performance data from this smaller set would then be used to provide high-confidence comparative evaluation from which to select the cycle or cycles for which pilot plant designs would be developed.

The ultimate objective of STCH was to provide a basis for commercial development and large-scale hydrogen production in support of the U.S. Hydrogen Economy Initiative. Accordingly, the prime metrics for transition to pilot plant design are those embraced by industry.

The Department of Energy, with industrial participation, applied considerable effort to develop guidelines that would assist in determining the commercial viability of thermochemical hydrogen production. These guidelines have changed over time and are even undergoing revision at the time of this writing. However, the production targets for central plant designs have proven useful in supporting quantitative comparative assessments for the cycles under study. The two principal metrics are cost of hydrogen per gallon-of-gas-equivalent (gge) at the plant gate and process efficiency, variously interpreted, but meaningfully defined as conversion efficiency of solar energy to hydrogen energy. Presently the Federal program is defining “efficiency” as the efficiency of conversion of solar-derived thermal energy to “lower heating value” hydrogen energy. The definition acknowledges implicit recognition that intercepted solar energy falling on the collection system is degraded by both thermal and optical losses through conversion to thermal energy to power the chemical processes. However, until these losses are included explicitly in the definition, the conversion efficiency of solar energy to hydrogen energy is violated. The original target schedules for high-temperature thermochemical production were changing during the period of evaluation and the progression (circa 2003 to 2008) is shown below (Table 1.1):

Target schedule transition	2012 → 2017	2017 → 2020
Cost target (\$/gge)	6	3
Process efficiency (%)	30	>35

Table 1.1 DOE Performance Targets

Phase 1 and Phase 2 selection processes are discussed in Section 2. The process for selection of candidates from Phase 3 cycles is discussed in Section 3. Technical status of the evaluated cycles along with path-forward recommendations or conditions that might lead to resumption of effort are summarized in Section 4. Summary discussion of the evaluation process, key challenges and recommendations are provided in Section 5.

STCH Historical Summary: The Solar Thermochemical Hydrogen Production Research Project (STCH) originated under Congressional direction to produce hydrogen in a closed chemical cycle using only solar thermal energy and water as feedstocks (Ref. Energy and Water Report). Research and development (R&D) was sponsored by the Hydrogen Research Program within the Office of Energy Efficiency and Renewable Energy (EERE) within the Department of Energy (DOE). STCH was initiated in 2003 and integrated work performed by the University of Nevada, Las Vegas (UNLV), the University of Colorado (CU), the General Atomics Corporation (GA), the National Renewable Energy Laboratory (NREL), Sandia National Laboratories (SNL) and the Argonne National Laboratory (ANL) under administration and management by the UNLV Research Foundation. Later, STCH became Solar Hydrogen Generation Research (SHGR) when photoelectrochemical hydrogen production (PEC) was added to the project by request of the Department of Energy. This report deals only with thermochemical processes and the acronym STCH will be used to reflect that part of SHGR managed for DOE by the UNLV Research Foundation and subsequently by the Department of Energy.

The UNLV Research Foundation announced its intention to terminate its technical management responsibilities during the period 2007-2008 and the Department of Energy decided to continue the effort initiated in 2003. Several new projects under grants managed by DOE's Golden Field Office were added to the inventory of active thermochemical cycle R&D with management transition to DOE. Some work continued to be managed by the UNLV Research Foundation through 2009 under no-cost extension decisions by DOE. Therefore, some of the work was managed under awards administered by the Golden Field Office for EERE, some was managed by the UNLV Research Foundation and some was managed by SNL through subcontracts funded under Sandia's Annual Operating Plan (AOP) approved by DOE Headquarters (DOE/HQ) in Washington DC. Coordinating this distributed effort was implemented via a consulting contract issued by the Golden Field Office with concurrence by DOE/HQ and with the cooperation of the UNLV Research Foundation. Following transition to DOE management, the project roster expanded to include SAIC in San Diego, CA and TIAX, LLC in Cambridge, MA. All other participants identified earlier continued under STCH until research priorities were formalized

through a DOE selection process. Presently all STCH work and the vast majority of PEC work are managed by the DOE.

2. Cycle Inventory Development and Initial Selection

Many hydrogen producing thermochemical cycles have been proposed over the last 40 years. A literature search was performed to identify all published cycles¹⁻⁵⁸. These were added to an existing database that had been compiled earlier to identify cycles suitable for nuclear hydrogen production⁵⁶. Additional cycles were contributed by other researchers, particularly Claude Royèr (private communication). A smaller scale survey was carried out by scientists at Centre Etude Atomique (CEA)⁶². All of these cycles had already been included in the developed inventory. More than 350 distinct cycles were identified and new ones were added as appropriate. Each cycle was assigned a process identification number (PID) and a process name for use in a database developed by the STCH project. Cycle elements and cycle chemicals were listed under cycle information to assist in database queries.

Initial screening was designed to restrict the number of cycles that qualified for detailed evaluation. The Phase 1 (screening) objective was not to identify the best cycle but to eliminate from consideration those processes that likely would not be worth the effort of a detailed evaluation.

The approach established screening criteria to discriminate against unlikely processes. Sixteen measurable criteria were devised for use in measuring the practicability of a cycle. The methodology defined a numeric metric for each criterion in the range of 0 to 10 for each cycle. Every attempt was made to make the criteria objective, which was possible in most cases. For example, toxicity rankings were taken from EPA and NIOSH publications. When a chemical is not listed in these compilations, a ranking for the chemical was assigned by an experienced chemist. This ranking was then used for the chemical for any cycle in which it is present. Whenever there was not a published ranking for a criterion, one was established based on the experience and expertise of the contributing members. The corrosiveness ranking stems from the rate of chemical attack on common engineering materials used in chemical plant construction.

Criteria could be weighted to emphasize competitive features like capital and O&M cost, development risk, environmental risk and sensitivity to unavoidable intermittency in solar energy. Additional criteria weighting was used to account for cycle compatibility with different

solar energy collectors: trough, tower and dish technologies. This along with a weighted average of the scores of the individual criterion would generate a composite score for the cycle.

The criteria used to screen the practicability of a thermochemical cycle can be broken down into four different general categories: i) economic considerations, ii) applicability to solar power system, iii) level of previous effort and iv) environmental and safety issues. The criteria are:

Economic Consideration

Criterion 1. Number of chemical reactions

As number of reactions increases, complexity, required separations and number of reactors increases.

Criterion 2. Number of separation steps

- solid-solid separations
- solid-liquid separations
- liquid-liquid separations
- gas-gas separations
- aqueous/non-aqueous

Gas-liquid and gas-solid separations were considered “easy” and were not included in the tally for the total separation step within each cycle.

Criterion 3. Number of chemical elements

The number of chemicals in a cycle indirectly reflects the complexity of the process as a greater number of species are involved and normally results in a more complex process.

Criterion 4. Abundance of chemical elements

Favorable cycles are those that employ common chemicals and elements since these would usually be less expensive and readily available in large quantities.

Criterion 5. Corrosiveness of chemicals

Chemicals were classified from least to most corrosive, based on their corrosiveness on common metallic materials of construction.

Criterion 6. Solids transport

Solids transport usually requires specifically designed machinery. Slurry suspensions are more readily moved with available hardware and is scored as liquid transport.

Solar Collector/Receiver Consideration

Criterion 7. Use of radiant heat transfer to solids

The transfer of heat to and from solids is increased for higher temperatures, so cycles with very high temperature solids are favored. This criterion uses variable scale for temperature ranges from below 900°C to above 1800°C.

Criterion 8. Temperature of high temperature endothermic step

The highest temperature of a cycle was compared to the optimal temperature range for a solar thermal system (Kolb,). If the highest cycle temperature was near the optimal temperature then a high point score was assigned to the cycle when paired with this device. The further away the temperature was from the optimal temperature, the lower the point score. Our screening analysis considered the applicability of four solar collectors:

- a. Trough – optimal temperature 375°C
- b. Standard tower – optimal temperature 525°C
- c. Advanced tower – optimal temperature 875°C
- d. Dish – optimal temperature 1125°C

Cycles that were not well matched to a solar device received 0 points on this particular criterion and were excluded from further assessment even though they had high scores from the other criteria.

Criterion 9. Compatible with thermal transients and/or diurnal storage

Previous Level of Effort for Candidate Cycle

Criterion 10. Number of literature papers

A higher number of papers published on a cycle indicates higher maturity of understanding than for cycles that have not been studied, suggesting that problems associated with it might have already been addressed.

Criterion 11. Scale of testing

Favorable cycles that have attracted support for larger scale testing like integrated lab scale, demonstration testing and pilot plant testing are likely to have improved chance of commercial success.

Criterion 12. Energy efficiency and cost

Evidence of cost and efficiency studies is indicative of greater levels of effort and maturity of development.

Safety and Environmental Consideration

Criterion 13. Acute toxicity to humans

This criterion considered “the most dangerous chemical” in a cycle, as determined for acute human exposure. Points were assigned to the IDLH (Immediate Danger to Life and Health) values found in the NIOSH (National Institute of Occupational Safety and Health) Pocket Guide to Chemical Hazards.

Criterion 14. Long-term toxicity to humans

This criterion considered “the most dangerous chemical” in a cycle, as determined by chronic long term human exposure. Points were assigned based on the REL (Recommended Exposure Limits) values taken from the NIOSH Pocket Guide to Chemical Hazards.

Criterion 15. Environmental toxicity

This criterion examined “the most dangerous chemical” in a cycle, as determined for environmental exposure, from EPA categories of reportable quantities discharged to the environment. These values were found in 40 CFR1, table 302.4 and Appendix A of part 355, and points were assigned accordingly.

Criterion 16. Reactivity with air or water

A chemical may be inert in an enclosed setting but may become very hazardous with an accidental exposure to air or water. This criterion took the sum of the NFPA (National Fire Protection Association) hazard ratings for flammability and reactivity with air & water, for each chemical in a cycle, and assigned points based on the highest sum.

The scoring scheme of each criterion, other than those derived from published ranking, was established after careful deliberation among the group members based on their technical expertise and practical experience. Therefore, some criteria scores are based on “expert opinion”. An archived list of criteria scores associated with the various solar technologies and used for cycle scoring can be found in the database developed by STCH. Other criteria scores can be entered and used to find other comparative rankings through the data base that can be found at www.shgr.unlv.edu although this website will not be maintained in the future.

The “development and operations” weighting factor was derived in two steps using a six-sigma methodology. First, the relative importance of each of the 16 criteria to the operation of a solar hydrogen production system was determined. Team members identified 5 factors which were essential in the development and operation of a solar thermal hydrogen production plant and they are i) capital cost, ii) operation and management, iii) development risk, iv) diurnal cycle and v) environmental risk. A multiplication factor (mp) between 1-5 was assigned to each of them based on their perceived importance to the development and implementation of a central production plant. Next, the relevance of each criterion with respect to the 5 operational factors was determined. A relevance value of 0, 1, 3 or 9 was assigned to each criterion according to its significance to the factor. The relevance value range and distribution were chosen to amplify numeric differences among selection criteria. The raw weighting factor for each criterion provides a measure of the criterion’s importance to a plant scale solar hydrogen production system. Table 2.1 lists the multiplication factor for capital cost, operations and management, development risk, variable and diurnal insolation and environmental risk along with the relevance of each criterion for these factors. The raw weighting factor, indicative of the importance of each criterion to plant development and operation is obtained by the sum of the products of the relevance factor and the multiplication factor.

Table 2.1 Relative importance of criteria to plant development and operation

		Capital Cost	O & M	Develop. Risk	Diurnal Cycle	Environ. Risk	Raw Weighing Factor
	IMPORTANCE (mp)	5	4	2	5	2	
1	Few reactions	9	3	3	0	0	63
2	Fewer steps	9	3	3	0	0	63
3	Fewer chemical elements	3	1	3	0	0	25
4	Abundance of elements	9	1	0	0	0	49
5	Minimize corrosive chemicals	9	3	9	0	3	81
6	Minimize solids flow	3	9	3	0	0	57
7	Use of radiant heat transfer to solids	0	0	0	9	0	45
8	Temperature compatible to solar source	9	0	3	0	0	51
9	Oxygen release from high temperature step*	9	3	1	9	1	106
10	Many Papers	0	0	9	0	1	20
11	Extensive testing	0	1	9	0	0	22
12	Basis for economic justification	0	0	9	0	0	18
13	NIOSH IDL	9	9	9	0	0	99
14	NIOSH REL/TWA t	3	3	3	0	0	33
15	EPA release/report limit	3	3	3	0	9	51
16	Not flammable/water reactive	3	1	1	0	1	23

Maximum temperature, use of hazardous materials, use of corrosive chemicals, the number of reactions and the number of separations were found to be the most important criteria.

Table 2.2 Solar-device criteria weighting factors

			Weighing Factor			
		Raw Weighing Factor	Trough	Low Temp Tower	High Temp Tower	Dish
1	Number of chemical reactions	63	6	6	6	10
2	Number of separation step	63	4	4	4	8
3	Number of chemical elements	25	0	0	0	0
4	Abundance of chemical elements	49	3	3	3	3
5	Corrosiveness of chemicals	81	7	7	7	7
6	Degree of solids flow	57	10	7	7	10
7	Use of radiant heat transfer to solids	45	0	0	8	4
8	Temperature of high temp. endothermic step	51	10	10	10	10
9	Compatible with thermal transients and/or diurnal storage	106	0	0	5	5
10	Number of Papers	20	2	2	2	2
11	Scale of test	22	2	2	2	2
12	Efficiency and/or cost figures	18	2	2	2	2
13	Chemical toxicity to human	99	3	3	3	3
14	Long term toxicity to human	33	0	0	0	0
15	Environmental chemical toxicity	51	3	3	3	3
16	Reactivity with air and water	23	0	0	0	0
	Maximum raw score		520	490	620	690
	Score multiplier		0.192	0.204	0.161	0.145
	Maximum Score		100	100	100	100
	Cut-off		30	35	50	55

A set of weighting factors specific to each criterion and for each solar device were assigned on the basis of concurrence and expert opinion. Based on the raw weighting factors and the expertise of the team members, weighting factors between 1- 10 were generated and assigned to each criterion for each solar device. Table 2.2 lists the solar-specific criteria weights.

The score multiplier was chosen to cast all scores in the range 0-100. It is obtained by assuming maximum score of 10 for each criterion and summing the product of the solar device weighting factor and criterion score. The score multiplier is 100 over the sum of products.

Table 2.3 describes the criteria score assignment scheme. Criterion 8 scores reflect proximity of the Maximum cycle temperature to the “sweet spot” temperature of the selected solar device.

Table 2.3 Criteria scoring scheme

No.	Criteria	CRITERIA SCORE										
		0	1	2	3	4	5	6	7	8	9	10
1	Number of chemical reactions	>4			4				3	2		
2	Number of separation step	>4		4	3		2	1	0			
3	Number of chemical elements	>4		4			3			2		1
4	Abundance of chemical elements											
5	Corrosiveness of chemicals											
6	Degree of solids flow	Batch flow of solids			Continuous flow of solid			Batch flow of gases/liquids through packed bed				Continuous flow of liquids and gases
7	Use of radiant heat transfer to solids	No high temp heating	Solid heated above 900°C	Solid heated above 1000°C	Solid heated above 1100°C	Solid heated above 1200°C	Solid heated above 1300°C	Solid heated above 1400°C	Solid heated above 1500°C	Solid heated above 1600°C	Solid heated above 1700°C	Solid heated above 1800°C
8	Temperature of high temp. endothermic step											see Appendix B
9	Compatible with thermal transients and/or diurnal storage*											O ₂ release from high temp. oxide
10	Number of Papers	1	2-3	4-6	7-10	11-15	16-21	22-28	29-36	37-45	45-55	55+
11	Scale of test	No lab. work			Test tube				Bench scale			Pilot scale
12	Efficiency and/or cost figures	No calculated efficiency			Calculated efficiency based on elementary reactions		Estimated efficiency with rough flowsheet		Calculated efficiency with detailed flowsheet			Detailed calculated cost
13	Chemical toxicity to human	IDEI >= 1 ppm U, Hg, As		0.001 < IDEL <= 0.01 ppm Ag, Pb, U (sol), Hg, Ni	0.01 < IDEL <= 0.1 ppm Co, U, V, Sb, Br ₂ , I ₂	0.1 < IDEL <= 1 ppm Cr, H ₂ SO ₄ , Cu, Mn, Sn, Cl ₂ , KOH, NaOH	1 < IDEL <= 10 ppm FeO _x , SO ₂ , HBr, Mo, HCl, C, H ₂ S	10 < IDEL <= 100 ppm NO ₂ , NH ₃ , CO	100 < IDEL <= 1000 ppm FeO _x , NH ₃ , Mo compds, H ₃ PO ₄ , Mn Compds, C	1000 < IDEL <= 10,000 ppm C, CO, Mo	10,000 ppm < IDEL <= 100,000 ppm CO ₂	Not a personnel hazard (N ₂)
14	Long term toxicity to human	IDEI >=0.001ppm As, Be, Cd		0.001 < IDEL <= 0.01 ppm Ag, Pb, U (sol), Hg, Ni	0.01 < IDEL <= 0.1 ppm Co, U, V, Sb, Br ₂ , I ₂	0.1 < IDEL <= 1 ppm Cr, H ₂ SO ₄ , Cu, Mn, Sn, Cl ₂ , KOH, NaOH	1 < IDEL <= 10 ppm FeO _x , SO ₂ , HBr, Mo, HCl, C, H ₂ S	10 < IDEL <= 100 ppm NO ₂ , NH ₃ , CO	100 < IDEL <= 1000 ppm FeO _x , NH ₃ , Mo compds, H ₃ PO ₄ , Mn Compds, C	1000 < IDEL <= 10,000 ppm C, CO, Mo	10,000 ppm < IDEL <= 100,000 ppm CO ₂	Not a personnel hazard (N ₂)
15	Environmental chemical toxicity	Category X (1 lb. reportable)		Category A (10 lb. reportable)		Category B (100 lb. reportable)		Category C (1000 lb. reportable)		Category D (5000 lb. reportable)		
16	Reactivity with air and water	>6	6	5	4	3		2		1		0

Cycle scores were obtained for each solar device by the sum of products of the device weighting factor and the consensus criteria score, multiplied by the score multiplier. Based on this method, 360 cycles were evaluated and 67 thermochemical cycles with the highest scores were selected for study under Phase 2.

One question that must be addressed was how well this type of process eliminates from the study those cycles with a low probability of success. Stepwise regression and rank correlation methods were applied to answer this question by staff at the Sandia National Laboratories. The results of this study showed that (1) the selected cycles were not highly dependent on criteria weights, (2) the screening process was robust and (3) was generally accurate in determining the most promising cycles for further analysis.

The 67 cycles with highest scores moved to Phase 2 in which the thermal efficiency of each cycle was estimated. Phase 2 work included application of HSC Chemistry Database to determine thermodynamic state variables consistent with phase equilibria for each reaction step in a cycle. A simplified flow chart was then developed for each cycle that included mass and energy balance and non-optimal heat recuperation. Aspen Plus™ software was used where necessary. The cycle thermal efficiency (η) was calculated by

$$\eta = -\Delta H^\circ_{25C}(H_2O(\ell))/[Q_{solar} + (W_s + \Delta G^\circ_T + RT \ln(\Pi a_p^{np}/\Pi a_r^{nr}) + nFE_{ov})/\eta_e] \quad (\text{Eqn.2.1})$$

where

$\Delta H^\circ_{25C}(H_2O(\ell))$ is the standard enthalpy of formation of liquid water,
 Q_{solar} is the net solar heat determined from the mass and energy balance,
 W_s is the amount of shaft work required, primarily compression work,
 ΔG°_T is the standard free energy of any electrochemical step,
 R is the universal gas constant
 T is the temperature of the electrochemical step,
 a_p are the activities of the products of the electrochemical step,
 np are the stoichiometric coefficients of the electrochemical reactants,
 n is the number of charges transferred in the electrochemical step,
 F is Faraday's constant,
 E_{ov} is the over-voltage of the electrochemical step, taken as 0.2 volts if no membrane is required and 0.4 volts if a membrane is needed,
 η_e is the efficiency of electrical generation, optimistically taken as 0.5.

The 67 top-scoring cycles were evaluated in this manner. Table 2.4 lists cycles and their estimated efficiencies that resulted from the Phase 2 evaluation. Table 2.4 does not include cycles whose efficiencies were estimated to be zero.

A cut-off efficiency of about 35% was chosen to keep the number of cycles moving to Phase 3 within a manageable number. Table 2.6 lists the cycles that met the 35% cut-off efficiency⁶⁴. Of the cycles in Table 2.5, Multivalent Sulfur was not investigated because of the number of difficult gas separations. Hybrid Cadmium was not investigated because it required an electrolysis step in addition to managing a volatile hazardous material. Iron Oxide was not investigated because either batch processing or solids flow management would be required. Metal Sulfate Cycles were investigated but hydrogen release could not be demonstrated and these cycles were abandoned⁶³. Cadmium Carbonate showed extremely poor kinetics in the hydrolysis reaction and was abandoned in favor of a Cadmium Oxide cycle. The Office of Nuclear Energy undertook Phase 3-like study of Sulfur Iodine and Hybrid Sulfur so that the original STCH Project invested detailed theoretical and experimental effort in 6 cycles.

Table 2.4 Listing of non-zero efficiencies for top-scoring cycles

PID	Cycle Name	Eff. (LHV)	PID	Cycle Name	Eff. (LHV)
110	Sodium-Mn-3	50.0	184	Hybrid Antimony-Br	30.6
106	High T Electrolysis	49.1	134	Cobalt Sulfate	29.9
147	Cadmium Sulfate	46.5	56	Cu Chloride	29.2
5	Hybrid Cd	45.1	114	Hybrid N-I	28.2
6	Zinc Oxide	45.0	62	Iron Bromide	27.7
182	Cadmium Carbonate	44.3	23	Mn-Chloride-1	26.6
2	Ni-Mn Ferrite	44.0	51	K-Peroxide	23.5
194	Zn-Mn Ferrite	44.0	61	Sodium-Iron	22.8
67	Hybrid Sulfur	43.1	185	Hybrid Cobalt Br-2	21.7
7	Iron Oxide	42.3	53	Hybrid Chlorine	21.6
191	Hybrid Copper Chlo	41.6	160	Arsenic-Iodine	21.2
149	Ba-Mo-Sulfate	39.5	152	Iron-Zinc	19.9
1	Sulfur-Iodine	38.1	103	Cerium Chloride	18.0
193	Multivalent Sulfur-3	35.5	26	Cu-Mg Chloride	17.4
131	Mn Sulfate	35.4	199	Iron Chloride-11	16.9
72	Ca-Fe-Br-2	33.8	200	Iron Chloride-12	16.9
70	Hybrid S-Br	33.4	104	Mg-Ce-Chloride	15.1
24	Hybrid Li-NO ₃	32.8	132	Ferrous Sulfate-3	14.4
201	Carbon Oxides	31.4	68	As-Ammonium-I	6.7
22	Fe-Chloride-4	31.0	129	Mg Sulfate	5.1

Table 2.5 Cycles that could move to Phase 3 detailed theoretical and experimental study

Cycle	PID	Efficiency %	Estimated Max T
Sulfuric Acid Cycles			
Hybrid Sulfur	67	43	900
Sulfur Iodine	1	45	900
Multivalent Sulfur	193	42	1570
Metal Sulfate Cycles			
Cadmium Sulfate	147	55	1200
Barium Sulfate	149	47	1200
Manganese Sulfate	131	42	1200
Volatile Metal Oxides			
Zinc Oxide	6	53	2200
Cadmium Carbonate: Cadmium Oxide	182: 213	52: 59	1600: 1450
Hybrid Cadmium	5	53	1600
Non-volatile Metal Oxides			
Iron Oxide	7	50	2200
Sodium Manganese	110	59	1560
Nickel Manganese Ferrite	2	52	1800
Zinc Manganese Ferrite	194	52	1800
Hybrid Cycles			
Hybrid Copper Chloride	191	49	550

3. Formal Cycle Evaluation and Research Prioritization

Scheduling and planning efforts were continuous throughout the original STCH project. The earliest schedule called for pilot plan design(s) to be completed in FY 2008. As funding levels failed to meet their targets, and as more understanding accompanied detailed study of the six Phase 3 STCH cycles, it became apparent that the original schedule would not be met. In a series of meetings with DOE representatives, a new schedule was agreed upon by both DOE and the initial STCH participants. This new schedule called for selection of the best cycle or cycles in FY 2009, to be accompanied by increased focus of resources on cycle particulars and implementation of on-sun demonstration in FY 2012. Data from focused research and development of a few cycles and from on-sun demonstration would be adequate to complete a pilot plant design.

It was during this period that the UNLV Research Foundation decided to terminate its management and administration responsibilities and the STCH research and development effort transitioned to DOE for all its management and administration. A decision to retain the schedule for selection of a few cycles for focused attention accompanied this transition. At the same time, there was another and serious interruption in planned funding. FY 2008 was funded essentially with carryover from allocations made in FY 2007 and the FY 2009 allocation was less than one-half the FY 2007 allocation. Consequently, work essential to a balanced comparative analysis of the STCH cycles was not completed.

Additional changes in the STCH cycle inventory accompanied the transition to DOE management and administration. The original Sodium Manganese cycle encountered unacceptable levels of water to recover aqueous NaOH and close the cycle. Moreover, 80% or less of NaOH was recovered experimentally in the hydrolysis step and the consequence of carryover was not known. However, DOE/EERE provided funds to explore direct thermal dissociation of NaMnO_2 and is consistent with the Non-volatile Metal Oxide Cycles although vaporized oxides of Na metal might be present. This cycle has been called the Sodium Manganate cycle. Another cycle, the Photolytic Sulfur Ammonia cycle, was introduced by DOE/EERE. This cycle is consistent with the Hybrid Cycles and became a part of the STCH inventory without participating in the initial cycle selection process. Finally, under sponsorship of the SNL-directed STCH effort, a ferrite process was introduced in which the ferrite material is synthesized using atomic layer deposition. This cycle became the ALD Ferrite cycle and is consistent with the Non-volatile Metal Oxide Cycles. Table 3.1 lists the cycles subject to evaluation in the DOE-directed formal evaluation process.

Table 3.1 Cycles considered in the formal evaluation process

Class	Cycle
Sulfuric Acid Cycles	Sulfur Iodine
	Hybrid Sulfur
Volatile Metal Oxide Cycles	Zinc Oxide
	Cadmium Oxide
Non-volatile Metal Oxide Cycles	Sodium Manganese and Sodium Manganate
	Nickel Manganese Ferrite
	ALD Ferrite
Hybrid Cycles	Hybrid Copper Chloride
	Photolytic Sulfur Ammonia

Nickel Manganese Ferrite did not participate fully in the evaluation and prioritization process because work on this cycle was fully funded by internal funds of the Sandia National Laboratories. Whereas a “watching brief” was maintained through cooperation of SNL, decisions regarding continuation and priority were reserved to SNL. As mentioned earlier, the Office of Nuclear Energy managed and administered thermochemical work on Sulfur Iodine and Hybrid Sulfur. However, DOE/EERE, through Savannah River National Laboratory and through Sandia National Laboratories provided support to integrate these cycles with a solar energy source and both cycles participated fully in the evaluation process.

Virtually all of these cycles were at different stages of R&D maturity at the time of the evaluation.

- Sulfur Iodine had progressed to implementation of an Integrated Lab Scale (ILS) test that was meant to demonstrate all steps with cycle closure using a lab thermal source instead of nuclear or solar. The ILS was never operated successfully. No reviewed H2A analysis of product cost had been completed at the time of the evaluation.
- Hybrid Sulfur had progressed to demonstration of an electrolytic step that nonetheless suffered from sulfur crossover and contamination and degradation of the membrane. No

integrated process demonstration had been performed. H2A cost analysis was in review but not completed at the time of the evaluation.

- Photolytic Sulfur Ammonia had reached the point of preliminary demonstration of all steps, but non-precious catalyst material had not been discovered for the photolysis step and thermal efficiency had not been established principally because conceptual system design issues remained unresolved. The same deficiency prevented completion of reviewed H2A analysis.
- Zinc Oxide had progressed in step-wise fashion (no closed or integrated cycle demonstration) to a point where a termination recommendation was made by the development team.
- Cadmium Oxide had progressed to demonstration of hydrolysis and CdO decomposition. The quench reaction was conceptually designed to minimize recombination but not demonstrated. No reviewed H2A had been completed at the time of the evaluation.
- Sodium Manganese had progressed in step-wise fashion to a point where a termination recommendation could be made on grounds of efficiency losses due to aqueous NaOH distillation. Work on a simplified sodium manganese cycle, although promising, was in its early stages. Using apparently reasonable assumptions, H2A analysis was performed but was not reviewed at the time of the evaluation.
- Nickel Manganese Ferrite did not participate fully in the process, but experiments seemed to indicate failure of the concept because of active material degradation under thermochemical cycling.
- Preliminary experimental work on the ALD Ferrite material suggested durability under thermochemical cycling, but kinetics and optimal operating temperatures were yet to be determined. Ferrite costs were estimated but not confirmed and active material durability was unknown for extended thermochemical cycling. H2A results were unreviewed.
- Hybrid Copper Chloride had not yet demonstrated an electrolysis cell design that did not degrade due to copper crossover. All other steps had been demonstrated but not optimized. H2A analysis continued to undergo revision and review.

Nonuniform state of progress among the cycles made the establishment of an objective and rigorous comparative framework unlikely. Objective metrics, like cost and system efficiency, for the majority of cycles would be based on assumptions and those assumptions would be made by cycle proponents, violating objectivity in the process. Whereas these assumptions could be (and were) discussed and criticized in the evaluation process, the critics would necessarily have been proponents of alternative cycles and objectivity would once again be violated. Rigor in the comparative assessment would require that metrics be developed for the same performance

characteristics for all cycles. Since the cycles varied so significantly in their development, it was difficult to establish rigorous performance metrics that would apply equally to all.

These obstacles to a rigorous and objective comparison framework led to the decision to base the evaluation on a qualitative framework designed to assess

- schedule and likelihood of demonstrating cycle technical feasibility
- likelihood that the cycle would (or would potentially) meet DOE cost and efficiency targets
- obstacles and proposed resolutions for the above two issues

An informal ranking process was proposed to develop consensus priority ranking of the candidate cycles according to

- projected performance in terms of DOE targets
- likelihood of overcoming R&D obstacles
- likelihood of meeting system/engineering requirements

but this ranking process was abandoned in favor of identifying critical path items for each continuing cycle for focused R&D investment.

As these criteria are essentially qualitative and judgmental in nature, it was decided to seek general consensus among the project members regarding the assessment topics. Essential information necessary to undertake the assessment and ranking was provided in the form of a white paper for each cycle that was distributed to the entire project team to assure all had the opportunity to engage technical and judgmental issues well before the evaluation meeting.

Points in the white papers were to be addressed in more detail in a formal presentation delivered during the evaluation meeting during which issues and questions could be brought up by members of other projects.

Specific evaluation elements were described for inclusion in the white papers and the presentations. Discussion points associated with each of the required elements were identified and provided to the authors, presenters and participants. The elements and associated discussion points are listed below:

- a. Cycle description in summary form with a block diagram describing the R&D pathway and milestones to meeting DOE targets.
 - i. Is the listing of technological strengths and weaknesses of the cycle comprehensive?
 - ii. Does the block diagram include all chemical reactions?
 - iii. Is there theoretical and/or experimental demonstration of cycle closure?
 - iv. Are side reactions and reaction yields for each step addressed?

- v. Are effects of recycled chemicals from reactions that do not go to completion addressed?
- vi. Is the R&D pathway comprehensive in describing all the development and testing necessary to assert cycle feasibility?
- vii. Is the milestone list comprehensive?
- b. Listing of proven and unproven pathway elements
 - i. Is the listing of proven and unproven pathway elements comprehensive?
 - ii. Are the proven pathway elements supported by data or literature citations?
 - iii. Are potential side reactions identified and demonstrated to be inconsequential?
- c. Listing of materials and component challenges accompanying a laboratory scale integrated demonstration
 - i. Have all materials and components requirements been addressed?
 - ii. Are all raw materials readily available?
- d. Summary of economic analysis using H2A with identified assumptions and uncertainties
 - i. Are the assumptions reasonable?
 - ii. Are all assumptions identified?
 - iii. Are the parametric ranges of uncertainties reasonable?
 - iv. Has the analysis package been reviewed and “approved” by TIAx, LLC?
 - v. What are the significant issues requiring resolution in the H2A analysis?
 - vi. Do projected hydrogen gate costs meet DOE targets (\$3/gge by 2017)?
- e. Cycle proponent recommendation to terminate or proceed
- f. If “proceed”, detailed research plan with workforce and budget requirements and schedule to resolve cycle performance and technology barriers necessary for integrated laboratory scale demonstration
 - i. Does the R&D plan address all issues relevant to integrated cycle demonstration?
 - ii. Are there critical elements of cycle performance whose resolution is “high risk”?
 - iii. Are workforce and budget requirements consistent with the R&D plan?
 - iv. Is the R&D team in place to complete the plan?
 - v. Is the schedule consistent with stated workforce and budget requirements?
 - vi. Is the schedule consistent with the DOE Program Plan?
 - vii. Are new facilities or new capital equipment required for a laboratory scale integrated demonstration?

- viii. What existing resources are available at other sites for a laboratory scale integrated demonstration?
- g. For transition to on-sun demonstration:
 - i. What new facilities are required for integrated on-sun demonstration?
 - ii. What existing appropriate resources are available at other sites for integrated cycle on-sun demonstration?

There are too many discussion points to address in this report. Instead of going through the discussion points individually, several are called out to address the most important issues that pertain to all cycles:

- Technical feasibility issues
 - theoretical and demonstrated cycle closure
 - side and incomplete reaction effects on efficiency or feasibility
- Integrated system concept design issues
 - effective materials of construction
 - component availability
- DOE performance target issues
 - cost projections for 2015 and 2025
 - thermal efficiency estimates for 2015 and 2025
 - principal uncertainties in projections/estimates

Table 3.2 (feasibility), Table 3.3 (concept design) and Table 3.4 (DOE target) list the principal respective issues for each STCH cycle identified from the submitted white papers and the presentations at the evaluation meeting. The evaluation process made it very clear that comparative assessment of the cycles under study could not be done with any level of certainty, mostly because of the different states of progress reflected in the submitted materials. This was not surprising since Photolytic Sulfur Ammonia R&D had been pursued for only about a year, compared with >5 years for Sulfur Iodine, Hybrid Sulfur, Hybrid Copper Chloride and Zinc Oxide; reactive ferrite had been under study for more than 5 years while ALD Ferrite had been active for less than a year. Sodium Manganese and Cadmium Oxide cycles had been under active investigation for about 3 years. In lieu of performing a comparative assessment accompanied by decisions to discontinue cycles, it was decided instead to redirect the R&D efforts for all cycles on those issues whose solutions would be essential to a continuation decision. The Zinc Oxide and Sodium Manganese proponent concluded on the basis of R&D and analysis results that these cycles were very unlikely to meet DOE targets even with continued support. It was recommended that these cycles complete necessary work to document their achievements and then to terminate further research and Development.

Issues pertaining to feasibility, concept design and performance that were common within a cycle are color coded to help with identification of the critical path items called out for emphasized R&D.

Table 3.2 Cycle feasibility assessments

Closure		Theoretical		Experimental		
Cycle	Theory	Experiment (stepwise)	Efficiency	Tech Feasibility	Efficiency	Tech Feasibility
Sulfur Iodine	yes	yes	metallic sulfur possible; HI decomposition	no sig. effect	non-ideal reactions; more data necessary	feasibility probably not affected but no demonstration
Hybrid Sulfur	yes	yes		depends on successful electrolyzer design	S crossover solution might increase bias or reduce current density	depends on successful electrolyzer design
Photolytic Sulfur Ammonia	yes	yes	possible catalyst deactivation	unknown	photolysis efficiency unknown	unknown
Zinc Oxide	yes	yes but incomplete Zn recovery	none	none	reduction yield loss by recombination	depends on adequate Zn metal recovery
Cadmium Oxide	yes	yes but incomplete Cd recovery	none	none	reduction yield loss by recombination	depends on molten Cd quench effectiveness
Sodium Manganese	yes	yes but incomplete Na recovery	mixed oxide kinetics/ composition unknown	side reactions might affect complete Na recovery	hydrolysis and reduction incomplete	carryover effects not demonstrated
ALD Ferrite	yes	yes	none	none	back reaction effects unknown	Durability under TCH cycling
Hybrid Copper Chloride	yes	yes	prevention of Cu crossover	depends on successful electrolyzer design	spent anolyte composition; Crystallizer performance unknown	depends on successful electrolyzer design

Table 3.3 Conceptual system design issues

Cycle	Block system	Aspen Plus™	Materials	Components
Sulfur Iodine	complete	yes	sulfuric acid concentrator heat exchanger	counter current Bunsen reactor; reactive distillation reactor; SPR heat exchanger
Hybrid Sulfur	complete	yes	sulfuric acid concentrator	electrolyzer; SPR heat exchanger
Photolytic Sulfur Ammonia	solar field and mirror choice	no	non-precious photocatalyst	beam-splitting optics; hot mirrors
Zinc Oxide	complete	yes	high temperature reactor materials	fluid wall reactor
Cadmium Oxide	solar system preliminary	yes	hydrogen separation membrane	fluidized bed decomposition reactor w/ quench; hight temp H ₂ transport membrane
Sodium Manganese	complete	yes	Na and Mx volatility could lead to deposits on and corrosion of reactor vessel material	oxygen transport membrane; hot particle heat exchanger; pneumatic particle transport system
ALD Ferrite	complete, but choice remains between fluidized bed, moving bed or stationary thin film reactor	no; might not be necessary	reactor materials of design; reactant material cycling stability	fluidized bed reactor or moving bed reactor
Hybrid Copper Chloride	complete	yes but not converged	hydrolysis and oxychloride decomposition reactors	electrolyzer; spent anolyte separator

Table 3.4 DOE performance targets issues

		Cost (\$/gge)	Efficiency (%)	Uncertainty
Cycle	2015	2025	2015/2025	
Sulfur Iodine	4.78 (2005)	5.77 (2015)	35/35	HI decomposition not demonstrated; sulfuric acid concentrator; efficiency
Hybrid Sulfur	4.80	3.19	33/33	Electrolyzer costs; sulfuric acid concentrator materials of construction; efficiency
Photolytic Sulfur Ammonia	5.73	NA	29/29	Cycle definition at the time of evaluation too uncertain for substantive analysis
Zinc Oxide	5.58	4.14	45/45 (from initial Phase 2 estimate; not reported in white paper)	Assumed 70% decomposition yield vs. 18% demonstrated; reactor materials of construction; oxygen transport membrane
Cadmium Oxide	3.94 (2005)	4.75 (2015)	40/40	Receiver cost and materials; quench feasibility and effectiveness;
Sodium Manganese	5.22	4.40	38/38	Oxygen transport membrane; recuperation from quench; particle heat exchanger materials; Na recovery
ALD Ferrite	3.45	2.91 (material cost estimated)	19/19	Ferrite cost and durability; process and component uncertainties; recycling rate
Hybrid Copper Chloride	4.50	3.45	39/41	Electrolyzer cost and effectiveness; reactor materials of construction; spent anolyte separation process

None of the cycles could present reviewed H2A analyses so that uncertainty persists for the cost estimates presented. Flowsheets for the multi-step processes were still undergoing optimization so that AspenPlus™ analysis of mass and energy flow balances were not finalized.

Consequently some degree of uncertainty persists for the thermal efficiency figures cited.

The evaluation process made it very clear that comparative assessment of the cycles under study could not be done with any level of certainty, mostly because of the different states of progress reflected in the submitted materials. This was not surprising since Photolytic Sulfur Ammonia R&D had been pursued for only about a year, compared with >5 years for Sulfur Iodine, Hybrid Sulfur, Hybrid Copper Chloride and Zinc Oxide; reactive ferrites had been under study for more than 5 years while ALD Ferrite had been active for less than a year. Sodium Manganese and Cadmium Oxide cycles had been under active investigation for about 3 years. In lieu of performing a comparative assessment accompanied by decisions to discontinue cycles, it was decided instead to redirect the R&D efforts for all cycles to those issues whose resolution would be essential for a continuation decision. Technical success in these identified topics would not in and of itself warrant continuation, but absent such success, the cycles would be either technically infeasible or economically uncompetitive. The Zinc Oxide and Sodium Manganese proponent concluded on the basis of R&D and analysis results that these cycles were very unlikely to meet DOE targets even with continued support. It was decided for these cycles that necessary work to document their achievements would be completed and no further research and development would be pursued, at least until additional information warranted resumption of effort.

It is evident from Tables 3.2-3.4 that many of the unresolved issues for the Sulfur Iodine and Hybrid Sulfur cycles would be managed by the Nuclear Hydrogen Initiative. These were not called out for prioritization by the formal evaluation. However, the integration of both cycles with a solar source was not defined with sufficient detail. Since both cycles planned to use the Solid Particle Receiver (SPR) under development by Sandia National Laboratories, effort under DOE/EERE support was directed to focus on integration of these cycles with the SPR. Additionally, the Sulfur Iodine, Hybrid Sulfur and Hybrid Copper Chloride teams were asked to collaborate in an effort to achieve commonality in their component and capital costing methodologies.

Photolytic Sulfur Ammonia had not yet achieved sufficient maturity to settle on a conceptual design since a choice between beam-splitting mirrors or dual solar fields had not been made. Serious uncertainty in the cost and effectiveness of beam splitting optics was generally evident during the evaluation. The proposed alternative was dual solar fields, with one to provide

thermal energy for ammonium sulfate reduction to produce ammonia and sulfur dioxide and the other to provide shorter wavelength radiation to drive photolytic oxidation of ammonium sulfite and produce hydrogen and ammonium sulfate. Accordingly, the Photolytic Sulfur Ammonia team was directed to acquire firm performance information and costs for beam-splitting optics and develop a design and cost estimates for a dual solar field architecture. Simultaneously, the team was directed to undertake preliminary investigation of a hybrid approach, replacing photolysis with electrolysis.

Zinc Oxide would be documented and further effort deferred until new information might arise that would argue for resumption of research and development. Economical means to suppress recombination during the quench of the ZnO decomposition step, possibly through use of a high temperature oxygen transport membrane, and identification of reactor materials capable of enduring thermal shock and operation at extremely high temperatures would be necessary for this cycle to become economically competitive. Additionally, demonstration of the proposed fluid wall reactor to prevent Zn loss by condensation on reactor surfaces would be necessary for cycle closure while demonstrated avoidance of sintering or other growth mechanisms affecting the size distribution of aerosolized Zn particles would be necessary to retain hydrolysis efficiency under cycling.

The Cadmium Oxide cycle suffers from recombination during quench of the CdO thermal decomposition step in ways very similar to the difficulties experienced by the Zinc Oxide cycle. Apart from the materials, the essential difference between the zinc and cadmium decomposition steps is that the zinc vapor quench is taken to solid zinc while the cadmium vapor quench is taken to molten cadmium, the material used in the hydrolysis step. Demonstration of the quench step for the Cadmium Oxide cycle had not been performed at the time of the evaluation so it was not possible to quantify the fraction of initial molten cadmium that would be re-cycled in the hydrolysis step. The process proposed for cadmium vapor quench was a rapid quench using either “cold” gas like carbon dioxide or molten cadmium spray as the quench medium. A cold gas quench is expected to nucleate molten cadmium droplets which then become condensation sites to further reduce cadmium vapor concentrations. Here, the number density of condensation sites can be crucial to effectiveness since higher number density generates higher surface to volume ratio causing greater surface recombination fraction. Molten cadmium droplet quench could be effective in reducing the number density of condensation sites but quench rate might be limited by thermal diffusion, causing significant recombination in the gas phase. The critical path issue for Cadmium Oxide was determined to be modeling the quench process to identify the optimum path and then demonstrate performance in laboratory scale experiments. A second

issue in this cycle is the relatively slow hydrolysis process whose kinetics, if not improved significantly by hydrolysis reactor design, could require much greater quantities of molten cadmium to be recycled in hydrolysis reactors to match throughput of the cadmium oxide decomposition step.

The mixed oxide sodium manganese cycle would be terminated after completion of work necessary to document achievements. This cycle suffered from a number of significant uncertainties, chief among which is economic recovery of sodium to close the cycle. Whereas incorporation of mixed metal ingredients like Zn-Mn and Zn-Fe improved sodium recovery without inordinate addition of water, the reaction did not go to completion, probably due to diffusion of Na and O into the MnO matrix. Moreover, side reactions like volatilization of NaOH or formation of other stable Na compounds introduced additional difficulty in assuring cycle closure. Na deposit was found on apparatus so this volatility problem would have to be resolved to move the cycle forward. The plant design incorporated significant transport of stored hot reactant solids and the cost of pneumatic transport over the ~25 km distance for solids (both hot and cold) instilled considerable uncertainty in plant capital and operating costs. These uncertainties when coupled with the projected hydrogen gate cost argued for termination of this cycle. An alternative cycle, direct thermal dissociation of NaMnO₂ (Sodium Manganate cycle) was proposed as a mixed volatility oxide cycle in which sodium manganate would be decomposed to MnO and vapor phase of Na_xO_y. The kinetics of the decomposition step is the primary barrier to operation of this cycle although there are several other obstacles, including performance of a fluid wall reactor and uncertainty regarding affinity of oxygen for sodium compounds relative to manganese. The project team was directed to evaluate the kinetics of the decomposition step preparatory for a later decision to continue or terminate.

The ALD Ferrite cycle was relatively immature at the time of the evaluation but is sufficiently simple that closure could be readily demonstrated in spite of residual uncertainty regarding back reaction extent which could affect performance sufficiently to prevent economic operation. However, performance would hinge crucially on the ability of the active materials to withstand repeated thermochemical cycling. If material characteristics are not stable under cycling, then the cycle might be abandoned, or it might be made more complex if a means could be found to restore initial active material characteristics. The team was directed to focus its attention on active material stability and durability preparatory to a subsequent decision to continue or terminate.

Table 3.5 Summary of evaluation outcomes

Cycle	Issues	Critical path focus
Sulfur Iodine	HI decomposition; acid concentrator heat exchanger; non-ideal chemistries; SPR	SPR integration
Hybrid Sulfur	acid concentrator; electrolysis membrane and cell design; SPR	SPR integration
Photolytic Sulfur Ammonia	Concept design; photolysis catalyst;	Beam splitting optics vs dual solar field; electrolysis option
Zinc Oxide	Recombination; reactor materials; fluid wall reactor; size distribution of metallic zinc	Document progress; terminate cycle R&D
Cadmium Oxide	Recombination; high temperature hydrogen transport membrane; beam down reactor cost	Quench modeling/demonstration; beam down reactor design and demonstration
Sodium Manganese	Na recovery; incomplete hydrolysis; reactant volatility;	Document progress; terminate cycle R&D
Mixed Volatility Sodium Manganate	Decomposition kinetics; effectiveness of fluid wall reactor; extent of back reaction;	Measure decomposition kinetics and back reaction
ALD Ferrite	Ferrite stability under extended thermochemical cycling; active material cost; back reaction effects	Evaluate ferrite stability under thermochemical cycling
Hybrid Copper Chloride	Electrolysis cell component materials and design; hydrolysis and crystallizer materials of construction; spent anolyte composition and separation membrane	Develop and demonstrate effective electrolysis membrane

Hybrid Copper Chloride has material issues for the hydrolysis and crystallizer reactors, likely resolvable at the appropriate time. Demonstration of material transfer from the crystallizer remains to be done, again likely to be successful. More importantly, quantitative composition of spent anolyte from the electrolysis process has not been determined and this step must precede the choice of membrane separation material for final processing of spent anolyte (aqueous CuCl and CuCl₂). However, until a satisfactory electrolyzer membrane and process have been

established, anolyte composition cannot be determined with any confidence. Electrolytic processing of fresh aqueous HCl with fresh aqueous CuCl produces hydrogen at the cathode and CuCl₂ in the anolyte. At the time of the evaluation, no electrolysis membrane had been discovered that was not degraded by transport and deposition on the membrane boundary of metallic copper. This causes degradation in performance and ultimately destruction of the membrane. Discovery of effective and durable membrane along with electrolysis cell design were identified as critical issues for resolution before a decision for continuation or termination could be made.

4. Cycle Status Summaries and Path Forward Recommendations

Status of the evaluated cycles at the time of the evaluation is reported here and reflects information reported in submitted white papers and presentations by cycle R&D teams. The summaries are not uniform in content due to contrast in cycle maturity and documents submitted by R&D teams.

4.1 Sulfur Iodine

The Sulfur Iodine Cycle is a three-step cycle (Fig. 4.1.1) that has been under development since ~1973^{2,7,40,45,54,56,57,59}. Research and development has been sponsored by the Office of Nuclear Energy under its Nuclear Hydrogen Initiative and Sulfur Iodine was selected for solar integration because it is a thermochemical process and its maximum temperature requirement is consistent with an advanced solar power tower. Each of the steps was demonstrated at laboratory scale but not all steps were optimized and an integrated lab-scale (ILS) demonstration was not successfully operated before termination. A week-long demonstration of the complete cycle was conducted in Japan but this was not a closed-loop demonstration, leaving open the question of reaction completion and effects of re-cycled reaction products.

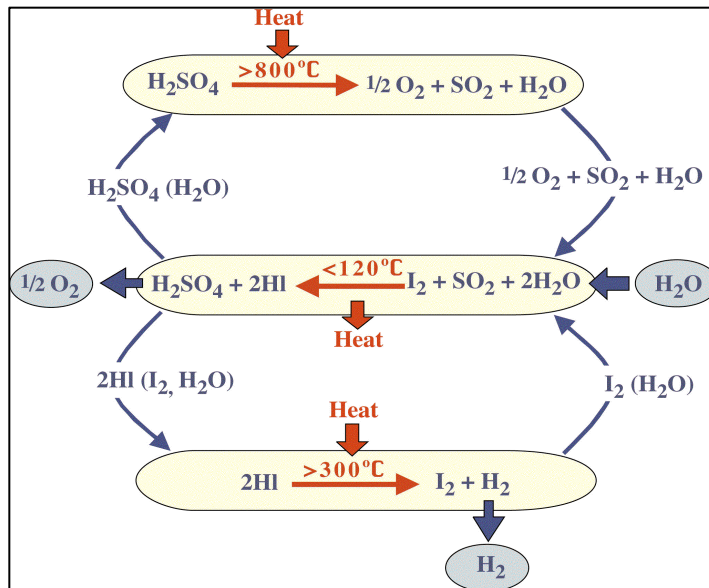


Figure 4.1.1 Sulfur Iodine three-step cycle

Concentrated sulfuric acid is reduced in the thermal decomposition reactor. Oxygen gas is released and aqueous SO_2 is reacted with iodine in the Bunsen reaction to produce sulfuric acid and hydriotic acid whose specific gravities are sufficiently distinct to permit gravimetric separation. Sulfuric acid is concentrated and recycled to the the decomposition reactor while HI is distilled to release hydrogen and the iodine is recycled for reuse.

Extractive distillation using phosphoric acid has been demonstrated but the process is slow and inefficient, requiring extended distillation column residence or recycling for recovery of expensive iodine. A reactive distillation step has been proposed that is anticipated to be more efficient but the process was not described in detail and had not achieved full laboratory demonstration so iodine recovery remains an issue. The Bunsen reaction does not appear to go to completion, giving rise to recirculated SO_2 whose consequence is unknown. A counter-flow reactor has been designed but not quantitatively demonstrated so the Bunsen reaction also remains problematic. Sulfuric acid concentration remains a materials challenge and the decomposition reactor (shown in Figure 4.1.1), while demonstrated, relies on multiple units (Figure 4.1.2) with a noble metal catalyst whose activity degrades with use and must be either cleaned or replaced, causing operational difficulty and expense.

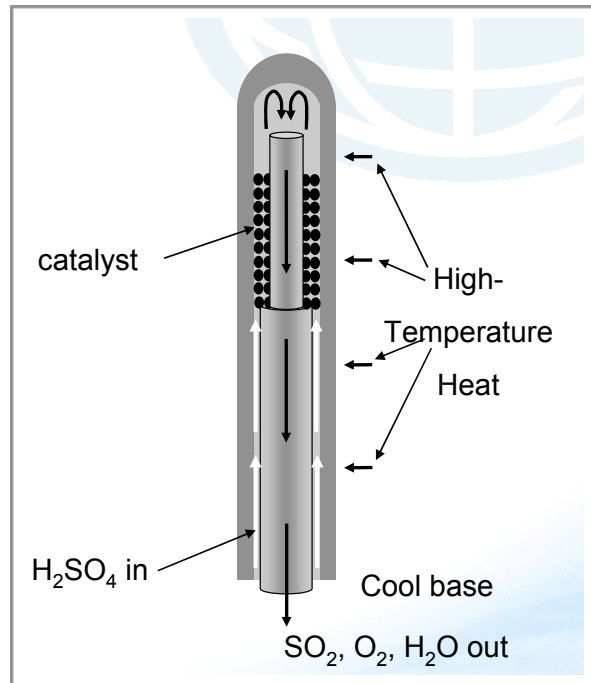


Figure 4.1.1 Bayonet decomposition reactor designed by Sandia National Laboratories

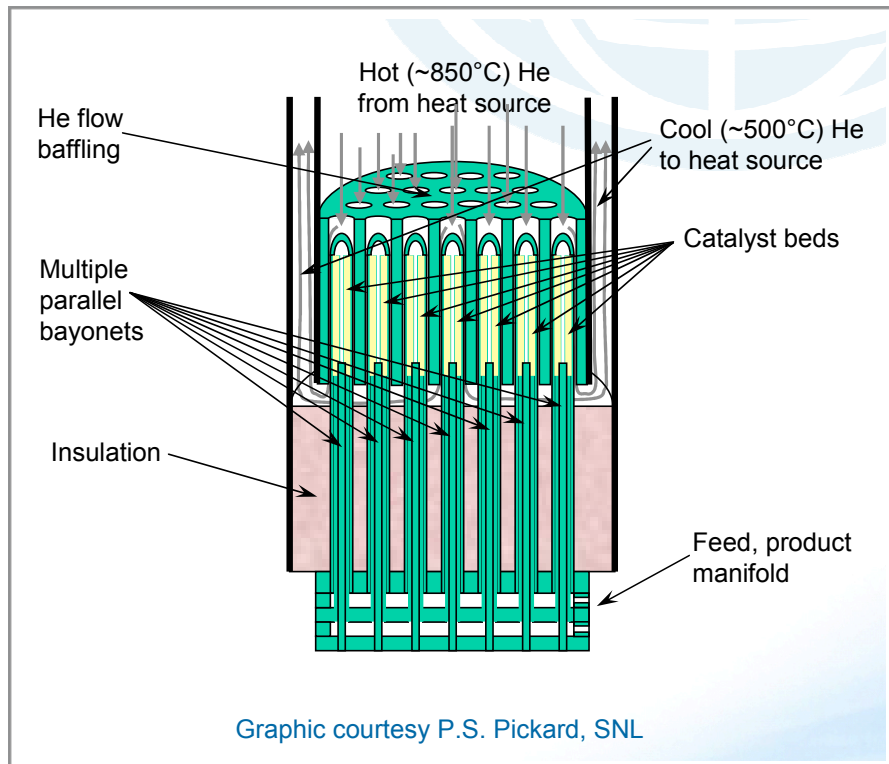


Figure 4.1.2 Bayonet decomposition reactor manifold designed by Sandia National Laboratories

A solid particle receiver was chosen to provide solar thermal heat for integration with the Sulfur Iodine cycle. The conceptual design called for particulate thermal medium to be heated by direct solar flux to about 1000°C and stored for use in the thermal decomposition reactor. The unknown consequence of hot particles impinging on the decomposition reactor led to implementation of an intermediate heat exchanger to provide either air or helium at 1000°C for heating the decomposition reactor. The particle medium is heated in the receiver section, stored in a hot storage vessel, used to heat the intermediate thermal medium and is then collected in a cold storage vessel. The particles are transported back to the solar receiver section by a bucket or auger system before recycling through the receiver and back to the hot storage vessel. This design concept has not been demonstrated and possibly serious difficulty could exist with durability of the particle thermal media and durability of an intermediate heat exchanger. The proposed solar interface schematic design is shown in Figure 4.1.3.

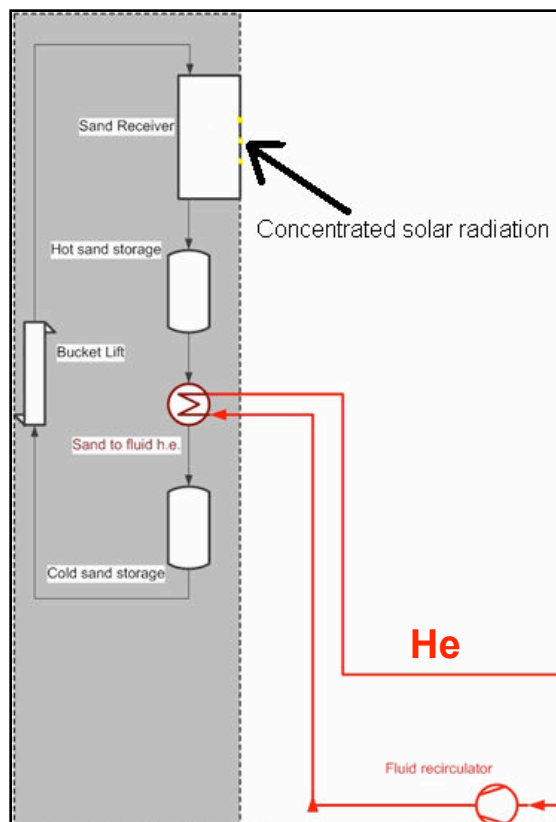


Figure 4.1.3 Schematic solar interface with the solid particle receiver with intermediate heat exchanger providing heated He gas to drive the decomposition reactor

Primary advantages and obstacles for the Sulfur-Iodine cycle are listed in Table 4.1.1.

Table 4.1.1 Sulfur-Iodine cycle advantages and challenges

Advantages	Challenges
Sulfur cheap and abundant	Iodine scarce and expensive
Liquid/gas stream; continuous flow process; separations are relatively easy	Corrosive chemicals
Thermal heat well-matched to advanced power tower	Non-ideal solutions prevent theoretical prediction of equilibrium states
Thermal storage concept is simple	Heat exchangers for solid particle thermal medium not demonstrated

A detailed flowsheet for the Sulfur Iodine thermochemical process was developed for the nuclear option. The thermochemical flowsheet for the solar option is identical. Simultaneous display of the entire flowsheet is not practical, so the process is divided into 3 sections:

1. Bunsen reaction section: $I_2 + SO_2 + 2H_2O \rightarrow 2HI + H_2SO_4$ (T $\sim 120^{\circ}C$)
2. Acid decomposition section: $H_2SO_4 \rightarrow SO_2 + H_2O + \frac{1}{2}O_2$ (T $> 800^{\circ}C$)
3. HI decomposition section: $2HI \rightarrow I_2 + H_2$ (T $> 350^{\circ}C$)

Sections 2 and 3 were optimized using AspenPlus™ software but lack of data and departure from ideal behavior of solutions in section 1 required a different model approach. Stream compositions and states were determined for each stream in the combined flowsheets and energy and mass balance calculations resulted in declared process efficiency of ~ 0.35 to 0.39 , depending on the heat exchanger medium, but the data were not listed from which these numbers were derived.

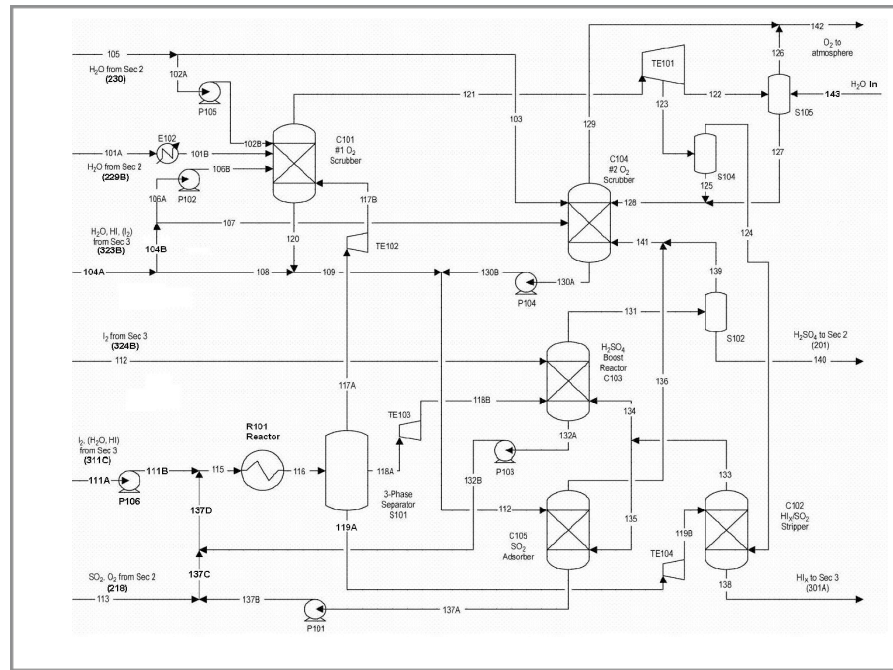


Figure 4.1.4 Bunsen reaction flowsheet (section 1)

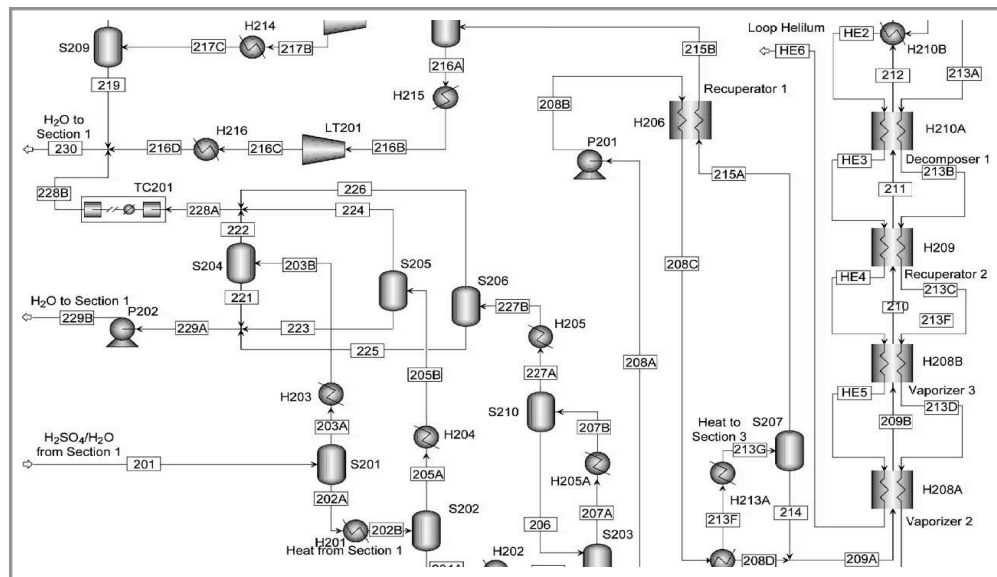


Figure 4.1.5 Acid decomposition flowsheet (section 2)

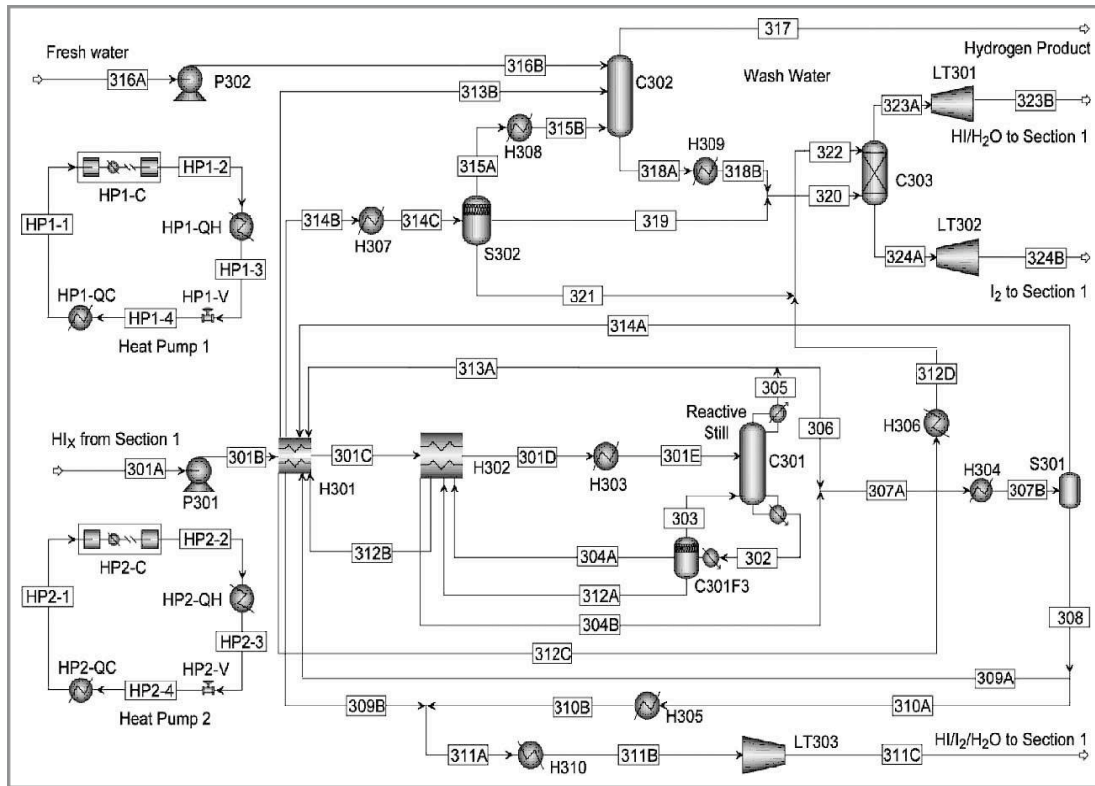


Figure 4.1.6 HI decomposition flow sheet (section 3)

Apparently, there was insufficient time to do serious cost analysis for the solar-powered Sulfur Iodine process so no reviewed H2A was available for comparison. The costs and efficiencies cited in Table 3.4 might change.

The path forward for the Sulfur Iodine cycle presented at the evaluation meeting engaged only the solar interface because NE was responsible for all other aspects of this cycle. Nevertheless, the issues identified above must all be resolved before the cycle can be considered for competition. The HI decomposition process is perhaps the most important issue because inefficiency in this step would likely increase cost beyond acceptable levels. The second most important issue is developing understanding of the equilibrium in the Bunsen reaction, unless it can be demonstrated that SO₂ carryover raises no obstacles to a closed cycle. Third, discovery of heat exchanger materials that can withstand the abrasive environment of a solid particle receiver is essential to either direct or indirect provision of thermal energy to the process. Finally, demonstration of operation of a solid particle receiver using an adequate thermal medium at the required temperatures and at scale sufficient to assure further scale-up is necessary.

4.2 Hybrid Sulfur

Hybrid Sulfur is a two-step cycle that uses high temperature heat ($\sim 900^{\circ}\text{C}$) to reduce sulfuric acid and an electrolysis step to oxidize SO_2 and restore the original oxidation state of the cycle. The Hybrid Sulfur cycle has been under development since before 1975 when the Westinghouse Corporation was issued a patent. Westinghouse demonstrated “closed-loop” operation in 1978 using an electrolysis cell designed and fabricated at Westinghouse so that both steps have been demonstrated but additional refinement remains necessary to optimize the cycle. The R&D was discontinued in 1983 but was resumed under the Nuclear Hydrogen Initiative^{1,2,4,5,10,15,16,18,19,26,30,43,59}. Fig. 4.2.1, taken from the team White Paper, illustrates the cycle. Research and development of this cycle

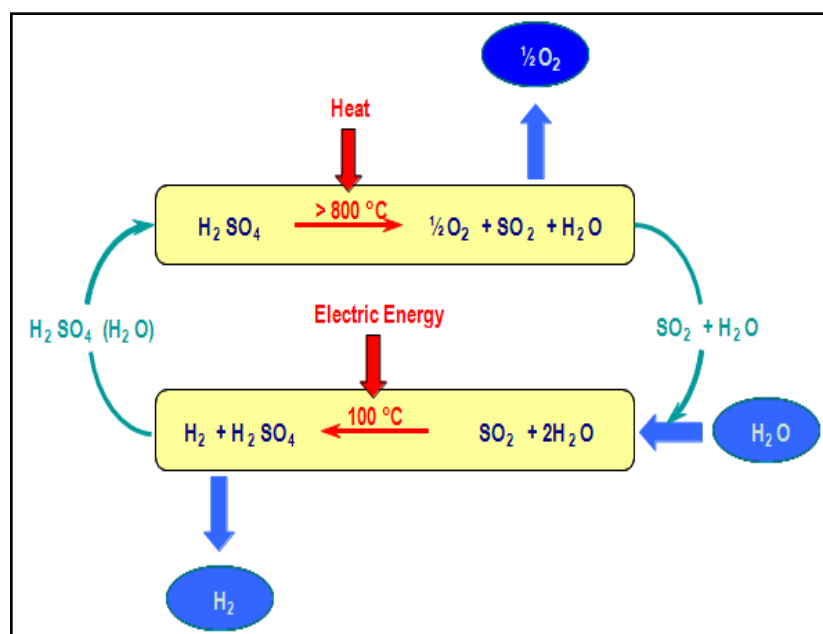


Figure 4.2.1 The Hybrid Sulfur cycle

has been sponsored by the Office of Nuclear Energy (NE) at DOE under its Nuclear Hydrogen Initiative and it was selected for solar integration because it is a thermochemical process and its required temperature is consistent with the optimal temperature of an advanced solar power tower. Oxygen gas is separated from the sulfuric acid decomposition products and aqueous sulfur dioxide is oxidized in the electrolyzer to release hydrogen gas and form sulfuric acid for recycle to the decomposition step. In practice, only about 40% of the SO_2 is electrolyzed and residuals are recycled through the electrolyzer with continuous feed of aqueous SO_2 from the thermal decomposition reactor. Dilute (~ 50 wt%) sulfuric acid from the electrolyzer is concentrated to about 75 wt% for feed to the thermal decomposition reactor.

The solar interface schematic for Hybrid Sulfur is the same as shown for Sulfur Iodine in Figure 4.1.3 and the decomposition reactor shown in Figs. 4.1.1 and 4.1.3 is also identical. The oxidation, however is accomplished electrolytically as shown in Figure 4.2.2.

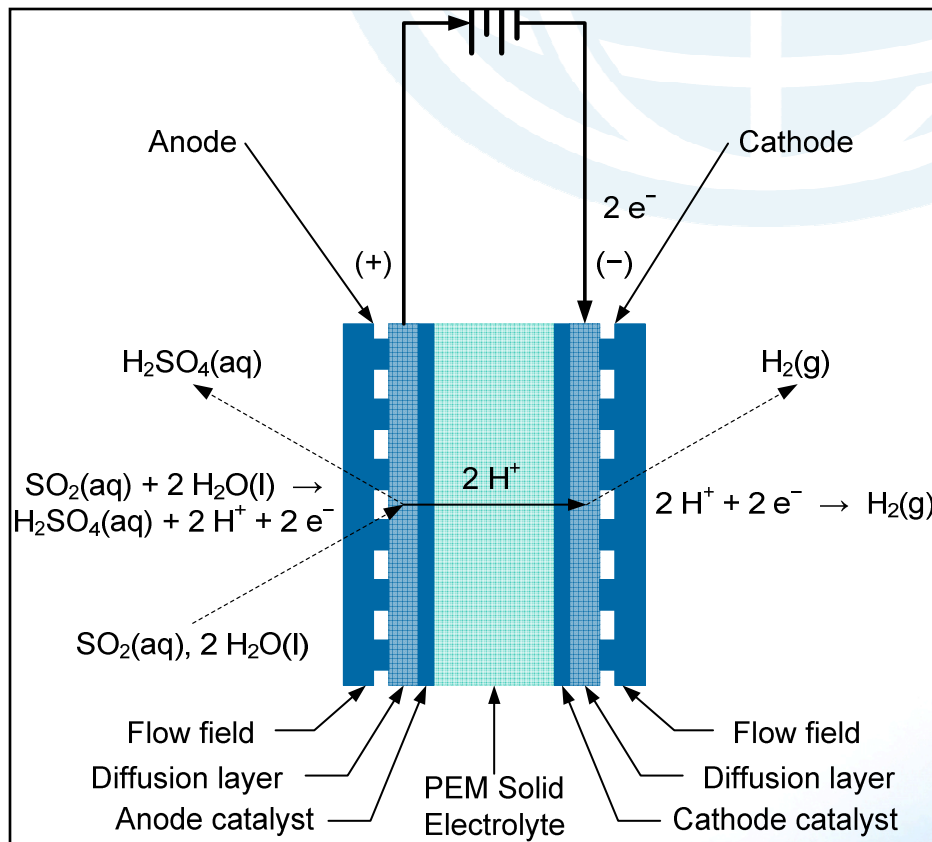


Figure 4.2.2 Schematic of PEM membrane in the Hy-Sulfur electrolysis step

The electrolysis cell has been demonstrated, but membrane permeability allows SO_2 diffusion to the cathode where reduced sulfur is deposited, degrading electrolyzer performance and, ultimately, membrane damage. This has been a key technical issue and no solution had been found at the time of the evaluation.

Hybrid Sulfur has the same advantages as Sulfur Iodine but has additional advantage owing to its simplicity. The obstacles are, however, somewhat different.

Table 4.2.1 Hybrid Sulfur advantages and challenges

Advantages	Challenges
Sulfur cheap and abundant	Corrosive chemicals
Continuous flow process; easy separations	Efficient cell design without sulfur deposition
Thermal heat well-matched to solar	Grid or solar electric power is required
Thermal storage concept is simple	Heat exchangers not demonstrated
Simple 2-step process	Solid particle receiver and sand

The Hybrid Sulfur flowsheet, shown in Figure 4.2.3, was designed to optimize integration between the decomposition reactor and the electrolysis cell and achieve maximum efficiency. More work could be invested to optimize the flowsheet to achieve minimum hydrogen cost to provide tradeoff analysis between cost and efficiency. SO₂ is dissolved in 43wt% sulfuric acid and fed to the anode of the electrolysis cell. Approximately 40% of the SO₂ is reacted, producing H₂SO₄ at 50wt% after electrolysis. H₂SO₄ is then concentrated to 75 wt% by two flashes in series (operating at 1 and 0.3 bar) and a vacuum column (at 0.13 bar). Oxygen separation is required before being extracted as byproduct.

The process efficiency was calculated with material and energy balances for the flowsheet in Figure 4.2.3 under the assumptions:

- Maximum process temperature 920 C
- Maximum process pressure 40 bar
- H₂SO₄ decomposition inlet concentration 75 wt%
- H₂SO₄ SDE inlet concentration 43 wt%
- Electrolysis cell temperature 100°C
- Electrolysis cell pressure 21 bar
- Electrolysis cell avg cell voltage 600 mV

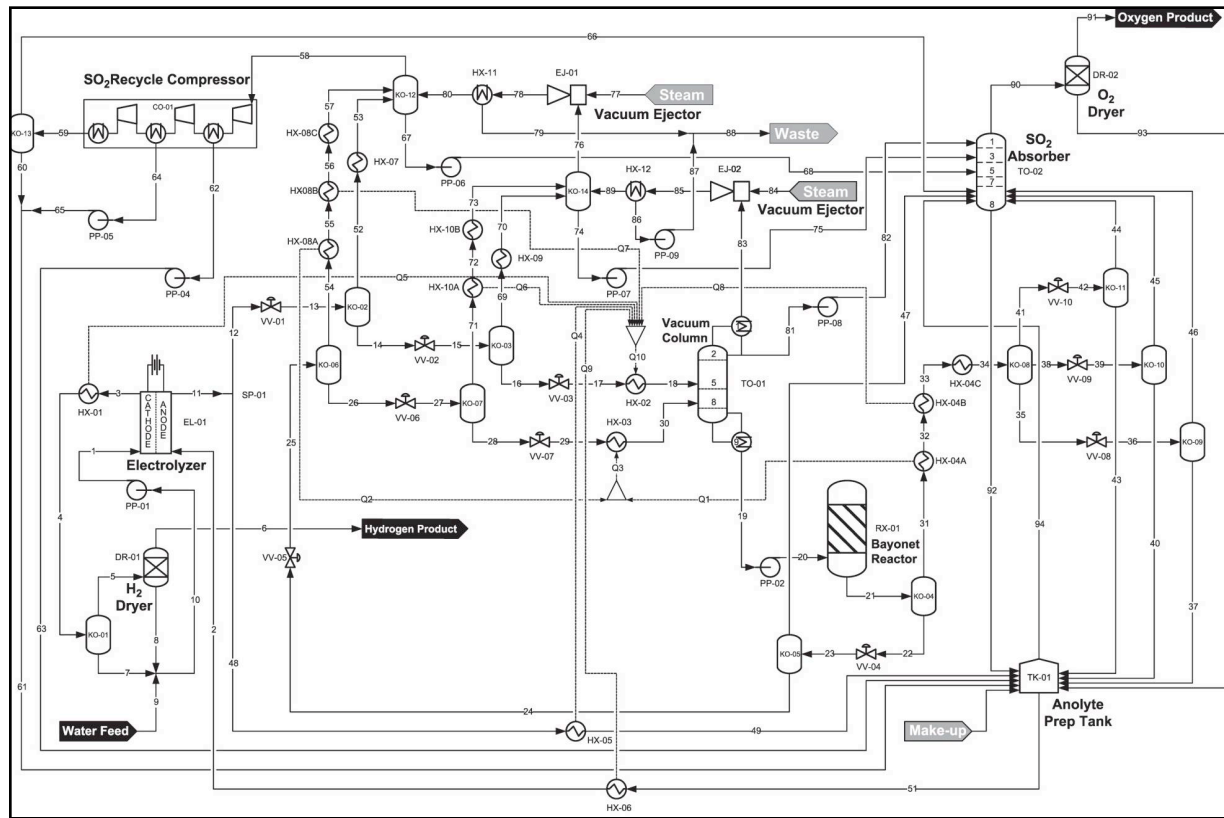


Figure 4.2.3 Hybrid Sulfur flowsheet

Calculated values for efficiency evaluation as reported in the process white paper are reported below:

Input:

- High temperature H₂SO₄ decomposition thermal power: 358 kJ/molSO₂ at some 950 C, which represents some 82% of the total thermal power needed to sustain the thermochemical process
- Low temperature thermal power for H₂SO₄ concentration: 75.5 kJ/molSO₂ at some 130 C, which is some 18% of the total external thermal power needed to sustain the HyS process
- Electric power for SO₂ oxidation: 115.7 kJ/molSO₂, which is almost 97% of the overall electricity needed for the HyS plant
- Electric power for HyS auxiliaries: 4.1 kJ/molSO₂, which is some 3% of the electricity needed for the thermochemical plant

Output

- H₂ production (LHV = 242 kJ/molH₂) at 21 bar and 100 C
- O₂ as byproduct

The process efficiency is calculated on the basis of the H₂ LHV and assuming a thermal- electric efficiency of 0.4 (H2A guidelines):

$$\eta = \frac{242}{358 + 75.5 + \frac{119.8}{0.4}} = 0.33$$

Cost analysis of the Hybrid Sulfur cycle was done for 2015 and 2025 in accord with assumptions and guidelines of the H2A analysis process. The plant was sized to produce annual average 100 tonne H₂/day with plant capacity of 0.75. An intermediate heat exchanger, used in the 2015 case, was replaced with direct heating of the decomposition reactor for the 2025 case. Helium transport allowed two heliostat fields and two towers to service a single process system in the 2015 case whereas direct heating of the decomposition reactor in the 2025 case required a single operational heliostat field and tower because transport of particulate thermal medium is difficult. The plant was equipped with hot storage providing 13 hours operation when off-sun. The H2A production costs for the tow cases are shown in Figure 4.2.4 with primary differences in decomposition reactor heating, heliostat cost reduction and electrolysis cell cost and performance improvements from 2015 to 2025.

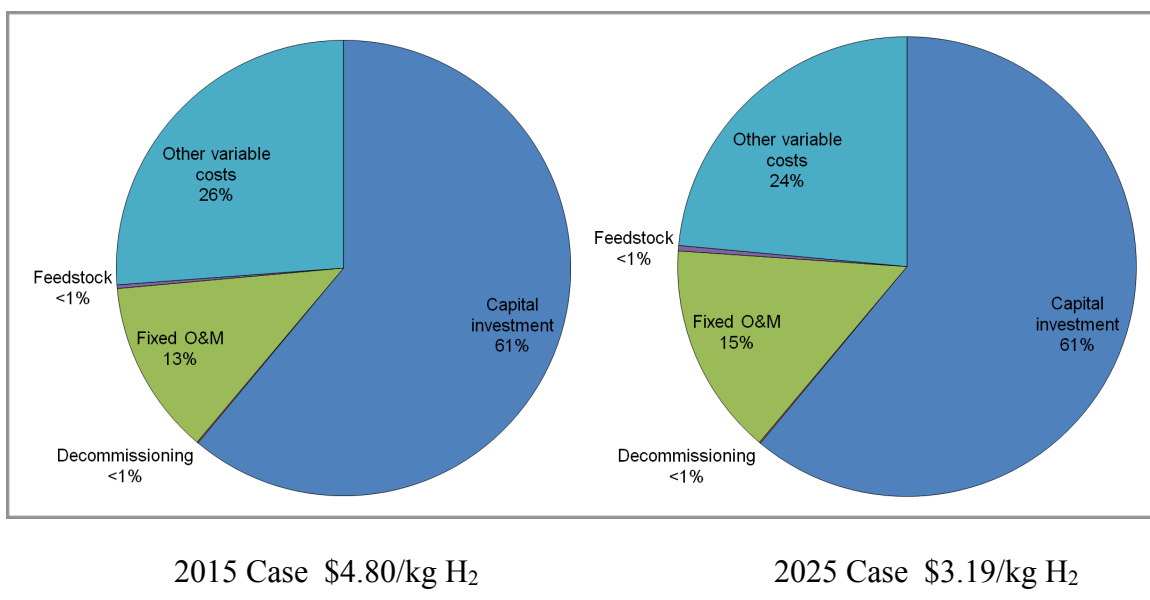


Figure 4.2.4 H2A hydrogen cost estimates for Hybrid Sulfur

The path forward for Hybrid Sulfur includes work that would be sponsored by both NE and EERE. Under the Office of Nuclear Energy the primary obstacle for successful operation was discovery of an electrolysis process and materials that would prevent SO₂ crossover and sulphur

deposit at the cathode. Under EERE, as for Sulfur Iodine, discovery of heat exchanger materials that can withstand the abrasive environment of a solid particle receiver is essential to either direct or indirect provision of thermal energy to the process. Finally, demonstration of operation of a solid particle receiver using an adequate thermal medium at the required temperatures and at scale sufficient to assure further scale-up is necessary.

4.3 Photolytic Sulfur Ammonia

The Photolytic Sulfur Ammonia cycle was presented as a four-step hybrid thermochemical cycle designed to make selective use of the solar spectrum with long wavelength spectral composition used to drive thermal processes and short wavelength spectral composition used to drive the hydrogen producing oxidation step using photolysis⁹. The cycle invoked intermediate thermochemical reduction steps to release oxygen. Figure 4.3.1 (taken from the team white paper) shows a schematic representation of the process in which it is evident that spectral beam splitting or dual solar fields would be required to power the process.

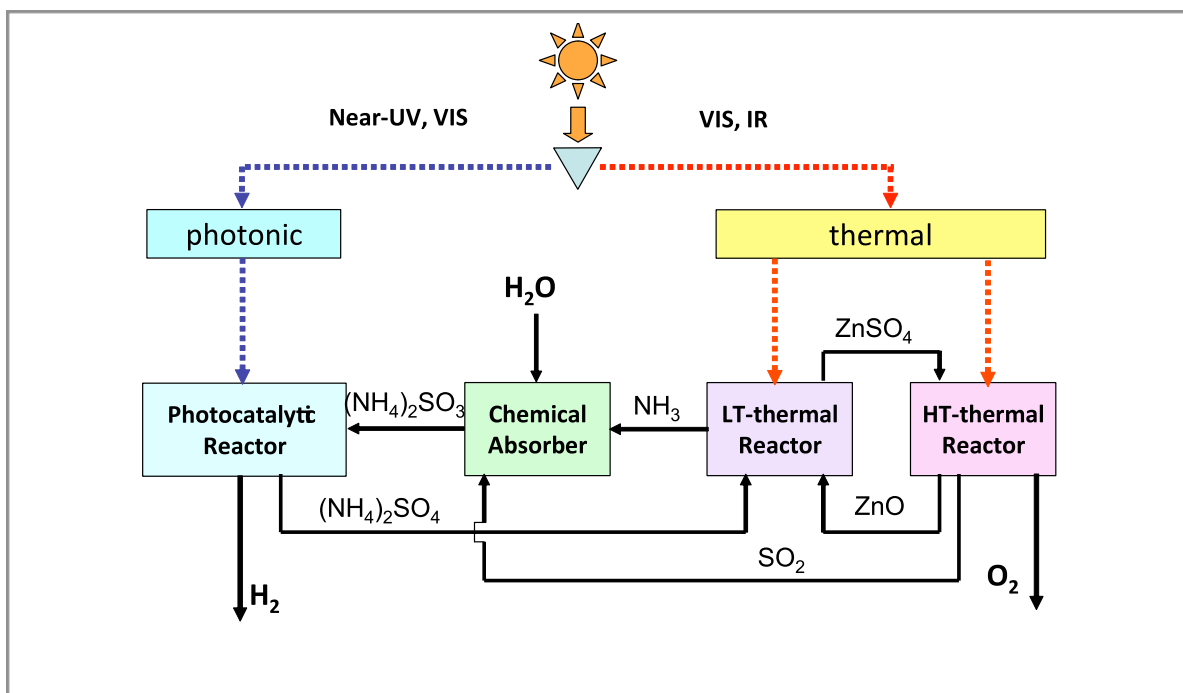


Figure 4.3.1. Photolytic Sulfur Ammonia schematic process

$\text{SO}_{2(\text{g})} + 2\text{NH}_{3(\text{g})} + \text{H}_2\text{O}_{(\text{l})} \rightarrow (\text{NH}_4)_2\text{SO}_{3(\text{aq})}$	120°C
$(\text{NH}_4)_2\text{SO}_{3(\text{aq})} + \text{H}_2\text{O}_{(\text{l})} + \text{h}\nu \rightarrow (\text{NH}_4)_2\text{SO}_{4(\text{aq})} + \text{H}_2$	80°C
$(\text{NH}_4)_2\text{SO}_{4(\text{s})} + \text{ZnO}_{(\text{s})} \rightarrow 2\text{NH}_{3(\text{g})} + \text{ZnSO}_{4(\text{s})} + \text{H}_2\text{O}$	500°C
$\text{ZnSO}_{4(\text{s})} \rightarrow \text{SO}_{2(\text{g})} + \text{ZnO}_{(\text{s})} + \frac{1}{2}\text{O}_2$	870-1000°C

Figure 4.3.2 Process chemistry for Photolytic Sulfur Ammonia

The cycle chemistry at the time of the evaluation is shown in Figure 4.3.2. The cycle team reported in their white paper that all steps had been demonstrated, all reactions went to completion and that there were no side reactions or unreacted products that carried over to the next step. The photolysis was carried out in the presence of a cadmium sulfide photocatalyst doped (or alloyed) with about 0.5 wt% Pt/Pd/Ru co-catalyst. The reported photolysis efficiency was about 0.29 as defined by the ratio of LHV H₂ generated to the energy of incident photons with wavelength less than 520 nm. These assertions apply only to laboratory experiments and the project plan shows continued work in all these areas. The issue of cost associated with noble metal catalysts was identified as a challenge, but not resolved. Difficulties, such as the solid-solid reaction of ammonium sulfate with zinc oxide to form ammonia and zinc sulfate, as well as transport of solids (zinc sulfate and zinc oxide) were identified as challenges, but design concepts had not progressed to the point that analysis and testing could be implemented. Similarly, options for solar field designs were offered (beam spectral splitting or dual solar fields) but specific designs were not developed at the time of the evaluation. As a consequence of these deficiencies, doubtless due at least in part to the short period of R&D before the evaluation, system efficiency calculations and estimates of hydrogen gate costs were without substance at the time of the evaluation and these are therefore not reported here.

Table 4.3.1 lists advantages and challenges for this cycle. Entries are taken liberally from evaluation materials submitted by the research team.

Table 4.3.1 Advantages and challenges for Photolytic Sulfur Ammonia

Advantages	Challenges
Separations are simple	Solids transport required
Ultra-high temperature not required	Coordinated operation of two reactors

Advantages	Challenges
Solar thermal spectrum applied to thermochemical steps; solar photolytic spectrum applied to photolysis step	Spectral splitting or dual solar field; either expensive or obviates photolytic advantage
Low cost photolytic reactor	Photocatalyst cost effectiveness

Figure 4.3.3 reproduces a flowsheet provided for the evaluation and description of its operation is also liberally taken from the cycle white paper. AspenPlus™ analysis was underway at the time of the evaluation but not completed.

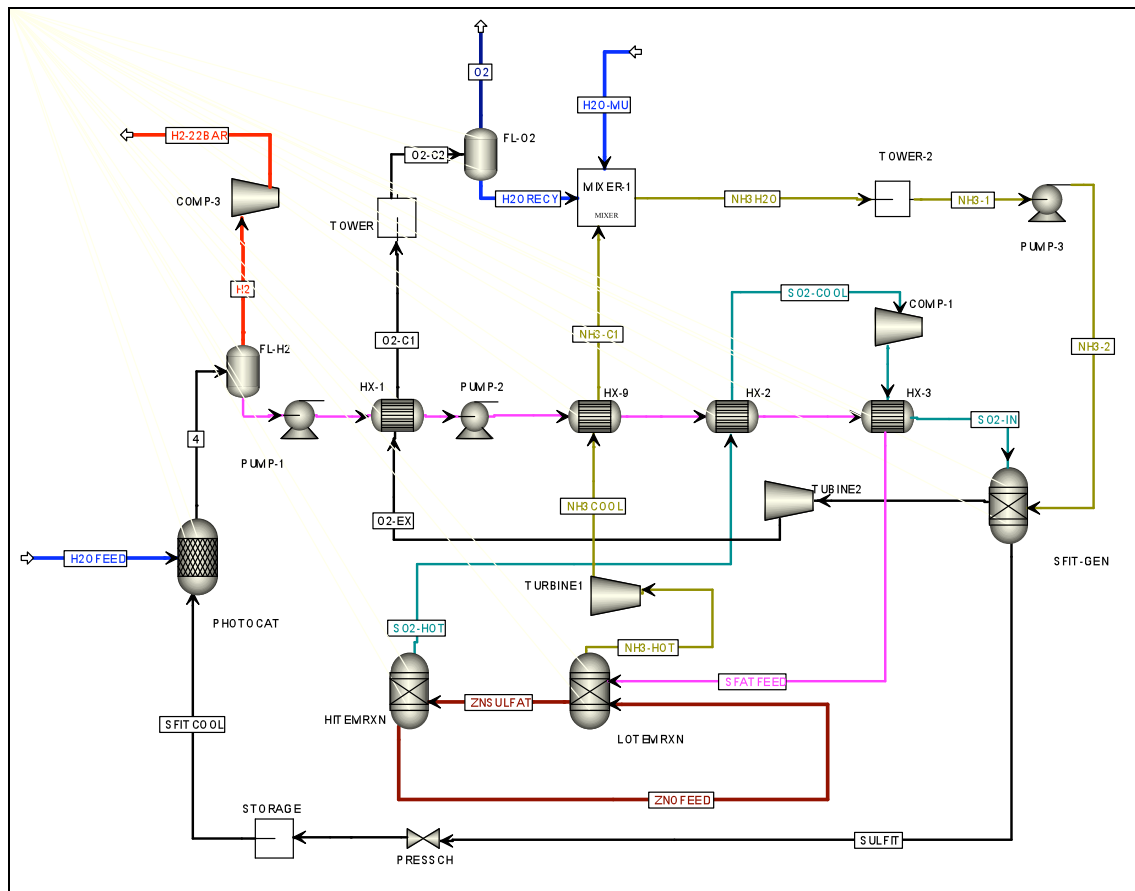


Figure 4.3.3 AspenPlus™ flow sheet for Sulfur Ammonia cycle

Hydrogen is produced at a rate of 11,199 kg/hr based on 12 hr/day operation in the PHOTOCAT reactor. In the photoreactor, ammonium sulfite ($(\text{NH}_4)_2\text{SO}_3$) and water react to produce H_2 and ammonium sulfate in the presence of a visible light activated photocatalyst. Hydrogen gas is separated from the aqueous ammonium sulfate ($(\text{NH}_4)_2\text{SO}_4$) solution by venting it from the

photoreactor (represented by the flash separation tank (FL-H2)). Aqueous ammonium sulfate solution is then pumped through a series of heat exchangers that preheat the brine before it is fed into the first solar thermolytic reactor LOTEMLRXN to release ammonia and form zinc sulfate. Hot product gases from this reaction (NH_3 and H_2O) are easily separated from solid zinc sulfate and allowed to expand in a turbine (TURBINE1) to generate electricity. The exit stream from TURBINE1 is sent to the heat exchanger HX-9 while the solid product ZnSO_4 is decomposed in HITEMRXN to release oxygen and form zinc oxide and sulfur dioxide. Hot gases SO_2 and O_2 enter heat exchanger HX-2 and are cooled by the ammonium sulfate stream entering LOTEMLRXN.

SO_2/O_2 and $\text{NH}_3/\text{H}_2\text{O}$ streams are reacted in SFIT-GEN producing aqueous ammonium sulfite and a moist gaseous oxygen stream. The aqueous products are collected in an above-ground tank (STORAGE) and allowed to cool down during the night - to be used later as a feedstock for replenishing the photocatalytic reactor. The oxygen stream $\text{O}_2\text{-EX}$ is further cooled in a heat exchanger HX-1 and cooling tower (TOWER). The moist oxygen leaving the cooling tower enters into a flash evaporator (FL-O2) which recovers condensed water and releases the oxygen into the ambient air.

Water H2ORECY collected in FL-O2 is combined with the makeup water and ammonia stream exiting HX-9 and sent to TOWER2 where it is condensed and fed into the sulfite synthesis reactor SFIT-GEN. The LOTEMLRXN and HITEMRXN reactions will most likely be carried out in a single solar receiver reactor – the design of which is still being worked on. The reaction in the photoreactor PHTOTOCAT will be conducted in a simple shallow (less than 1"), Kynar (or other suitable UV-VIS transparent material) covered flat bed unit illuminated by sunlight. The photolyte is continuously pumped in and out of the photoreactor(s). LOTEMLRXN, HITEMRXN and SFIT-GEN have been simulated using Rgibbs model. In the present flow sheet, PHOTOCAT is simulated using a stoichiometric reactor model. A ratio of about 10 moles of H_2O per mole of $(\text{NH}_4)_2\text{SO}_3$ has been assumed in the simulation.

The cycle white paper cited tower and heliostat cost at about 48% of capital cost whereas virtually all other cycles find the solar system comprising about 70% of capital cost. Since either specialized heliostats or dual solar fields would be required, it is difficult to reconcile the quoted solar costs in the white paper. Accordingly, the H2A results are assumed to be so preliminary that they will not be reported here.

The prime rationale for the photolytic process was founded on more efficient use of solar power by applying the shorter wavelength spectral component to photolysis and the longer wavelength component to thermal processes. The only way to realize this benefit is to split intercepted solar radiation into these components and direct the split beams to their respective tasks. A dual field realization does not use intercepted radiation more efficiently since the thermal component will be useless for the photolysis process and the photoactive component will not add materially to thermal processes. Consequently, discovery of a cost effective means of spectral beam splitting is mandatory for the Photolytic Sulfur Ammonia cycle to be continued.

4.4 Zinc Oxide

The Zinc Oxide cycle is a two-step volatile metal oxide cycle that has been under development since before 2003. In its simplest form, the metal oxide is reduced at a high temperature of about 2000°C, quenched to zinc particles and oxygen is released. The zinc is recycled and exposed to water vapor at about 425°C to release hydrogen and form ZnO^{51,52,61,62,65,66,67,71,72}:

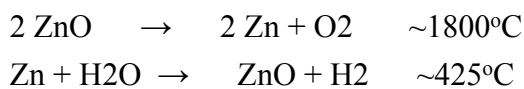


Figure 4.4.1 Zinc Oxide cycle chemistry

Four issues have driven the cycle development. First, the reduction step temperature generates serious difficulty in finding reactor materials of construction that are durable under operation. It was found that introduction of an inert gas, argon in experiments, would reduce the operating temperature to about 1750°C, but separation of argon from the oxygen is problematic since even a high temperature oxygen permeable membrane would suffer from either condensation or physical deposition of zinc particles in the pores.

Second, the zinc oxide decomposition step is limited in efficiency because quench is accompanied by significant recombination. Only 18% of zinc metal has been recovered under rapid quench whereas up to 70% and 85% recovery have been cited in analytic studies. It is speculated that recovery could be improved by quenching with fine zinc metal particles, but this approach would likely lead to larger zinc particles, reducing the effectiveness of the hydrolysis step. At this time, no process other than rapid quench has been found to reduce significantly recombination and thereby improve metal recovery. However, rapid quench reduces sensible heat recuperation for the cycle, thereby decreasing cycle efficiency.

Third, the oxidation (hydrolysis) step is limited by surface area of zinc metal since formation of the metal oxide on the surface inhibits further oxidation of the underlying metal. The higher the particle surface to volume ratio, the higher the efficiency of the hydrolysis process so that sub-micrometer zinc particles are necessary. Rapid quenching of the reduction step does produce very small particles, but efficient recovery has not been demonstrated and a closed cycle demonstration has not been attempted.

Finally, a porous flow-through wall was proposed to counter loss of zinc metal to condensation and particle deposition on reactor walls. The fluid wall concept has been used in other chemical processes but has not been demonstrated for the zinc cycle. A fluid wall reactor would require additional gas separation and would doubtless increase costs.

Table 4.4.1 Advantages and challenges for Zinc Oxide

Advantages	Challenges
Simple 2-step process	Extremely high temperature limits materials choice
Reactant materials abundant, safe and relatively cheap	Recombination limits efficiency
Continuous operation through Zn metal storage	Particle size limits hydrolysis efficiency
Variable insulation easily managed by oxide feed to reactor	Zn deposition on reactor walls and components
	High temperature oxygen transport membrane

The process flowsheet for a plant sized to produce annual average 100 tonne H₂/day with capacity factor 0.75 is shown in Figure 4.4.2. For the 2015 case study, a 3:1 molar flow rate of Argon:ZnO was assumed, ZnO decomposition was assumed to proceed at ~1750°C to 70% conversion, hydrolysis was assumed to be 100% efficient, and a 3-stage vacuum swing absorber (VSA) was used for Ar/O₂ separation. Quench sensible heat between 1800°C and 900°C is consumed and it is assumed that sensible heat between 900°C and a recovery temperature is recuperated. A dual multi-tube aerosol transport reactor⁷⁵ of siliconized graphite was configured with porous wall to maintain flowing Ar between Zn and ZnO gases and the reactor walls. The

2015 reaction was executed at atmospheric pressure so that compression is required to provide H₂ at 300 psig at the plant gate.

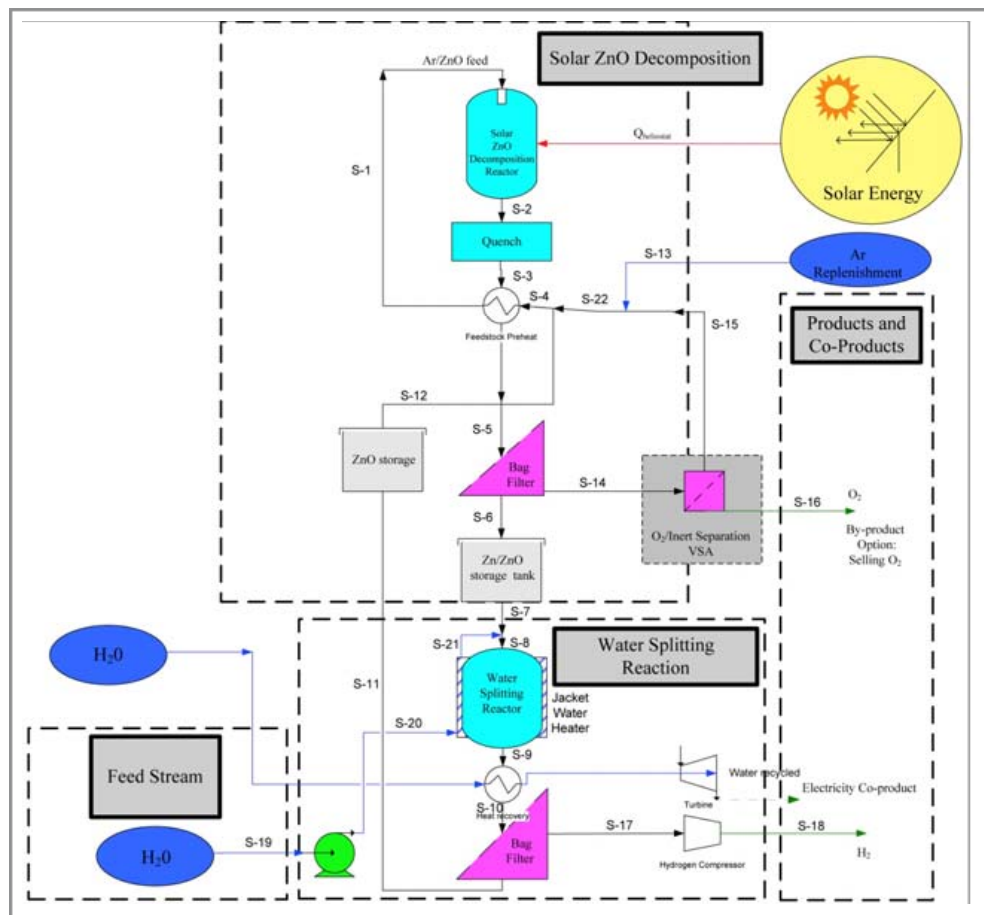


Figure 4.4.2 Zinc Oxide cycle flowsheet (CU Final Report)

The 2025 cast study assumed a single pressurized (300 psig) multi-tube reactor, 85% conversion efficiency for the decomposition step and a single stage VSA.

Three heliostat fields illuminated a 250 m tower and 13 hours of thermal storage (Zn metal) were maintained to allow continuous operation (weather permitting). The 2015 case required 15 towers to provide annual average production of 100 tonne H₂/day, while the 2025 case required 14 towers. Each heliostat field for both case studies contained 358 heliostats in about 3 acres and delivered 123 MWth to three secondary concentrators on each tower. The secondary concentrators delivered 112 MWth to each receiver.

The team calculated efficiency of solar energy to Lower Heating Value hydrogen energy so that the calculated ZnO efficiency values will be lower than the differently defined efficiencies requested by the program office. The 2015 efficiency was 17.2% while the 2025 efficiency was calculated to be 20.7%. The main causes of efficiency increase are increased decomposition yield (85% for 2025 and 70% for 2015), operation at gate pressure of 300 psig for 2025 instead of atmospheric pressure for 2015, and reduced argon inert gas use in 2025 so that a single stage VSA could be used instead of the 3-stage VSA used in the 2015 case study.

Capital cost allocations are shown for case studies 2015 and 2025 in Figures 4.4.3 and 4.4.4. The baseline gate cost for hydrogen in 2015 was \$5.58 /gge H₂ and could conceivably reduce to \$4.47 /gge H₂ with aggressive reduction in heliostat and tower costs accompanied by reduced cost for the receiver/reactor. 2025 baseline cost was found to be \$4.14 /gge H₂ and with similar aggressive component cost reductions could conceivably reduce to about \$3.46 /gge H₂. Since these cost figures did not appear to be reducible to meet the projected cost targets, the Zinc Oxide cycle was not recommended for continued development.

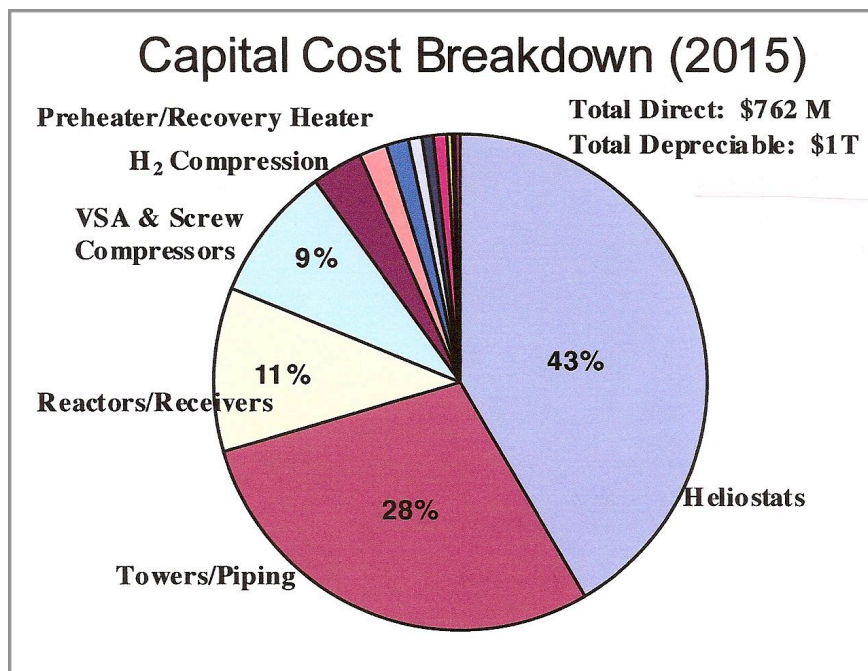


Figure 4.4.3 Plant cost allocation for the 2015 case study

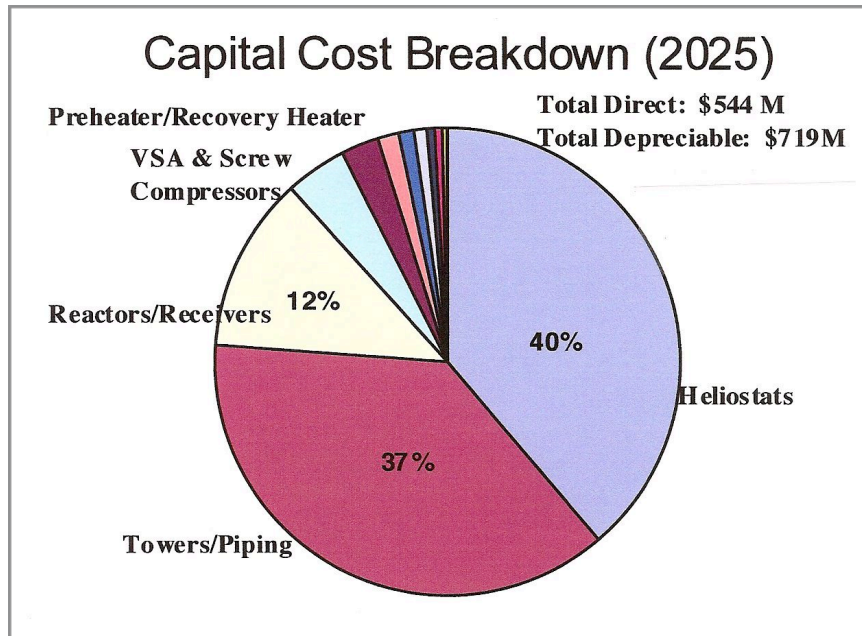


Figure 4.4.4 Plant cost allocation for the 2025 case study

The Zinc Oxide cycle development is unlikely to be continued without discovery of reactor materials capable of withstanding thermal shock and fatigue. Moreover, product cost is unlikely to meet targets without significant reduction in heliostat and tower costs well beyond those projected for the foreseeable future. Efficiency improvements are unlikely in the absence of methods for recuperating the sensible heat lost to rapid quench, and demonstration of ZnO decomposition yield of zinc metal near 70% is necessary to seriously consider resumption of development.

4.5 Cadmium Oxide

The Cadmium Oxide cycle is a simple two-step volatile metal oxide cycle^{21,24,29} with many similarities to the Zinc Oxide cycle. Primary differences are that the decomposition temperature is significantly lower for CdO, ~1450°C, the quench process proceeds to molten Cd instead of the solid metal product for ZnO, the proposed rapid quench is facilitated by use of molten Cd droplets as opposed to expansion through a cooled orifice as used by ZnO and the chemical plant is operated on the surface under a beam down solar collector design. Other important differences are the use of hazardous Cd as opposed to nonhazardous zinc in the two processes. The Cadmium Oxide cycle chemical steps and conditions are shown in Figure 4.5.1.

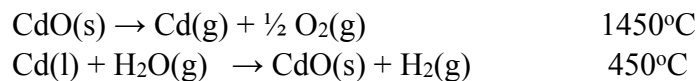


Figure 4.5.1 Chemical steps of the Cadmium Oxide cycle

As in the Zinc Oxide cycle, a third non-chemical step, quenching the decomposition products rapidly, is necessary to reduce recombination or back-reaction that reduces cadmium yield and recycles CdO to the hydrolysis step. A conceptual flow diagram for a process designed to operate 24 hours per day was developed and is shown in Figure 4.5.2.

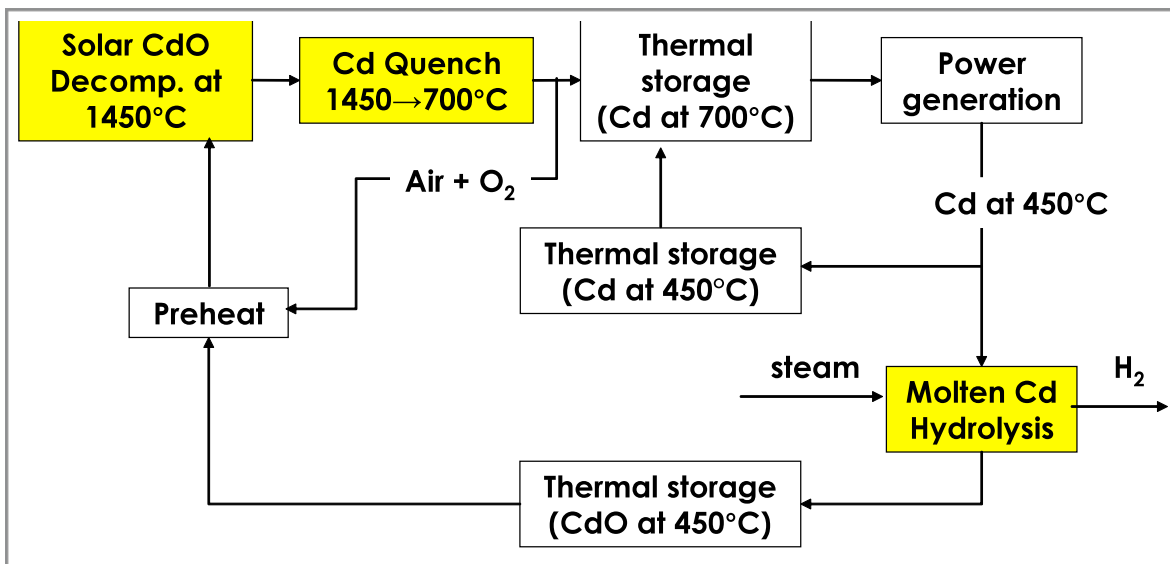


Figure 4.5.2 Process flow for a diurnal solar cadmium oxide hydrogen cycle.

Thermal storage and power generation are options included in the conceptual design. A third option reduces the decomposition temperature by incorporating inert gas flow with CdO in the decomposition reactor. O₂ and the inert gas can be separated readily from the quenched product but the inert gas would require separation for recycling. Replacing the inert gas with air is possible, but increase in O₂ partial pressure would likely make the quench less effective. Inert gas use has not been analyzed to determine if the temperature reduction is worth the additional separation required. Analysis of the CdO cycle without inert gas provided a thermal efficiency estimate of 59% (LHV).

Whereas the thermal efficiency of the CdO cycle is among the highest of all cycles considered, there remain difficult obstacles in the chemistry as well as in plant operations. Just as with the zinc cycle, recombination will limit the effectiveness unless it can be shown that rapid quench

either with or without molten cadmium nucleating sites provides high yield of Cd metal for recycling to the hydrolysis step. Moreover, hydrolysis of molten cadmium is rate limited due both to chemical kinetics and to accumulation of CdO on the molten Cd surface. A rotating kiln counter flow hydrolysis reactor design was designed for increasing the hydrolysis yield through mixing and residence time selected (through kiln dimension and orientation) to react all molten cadmium.

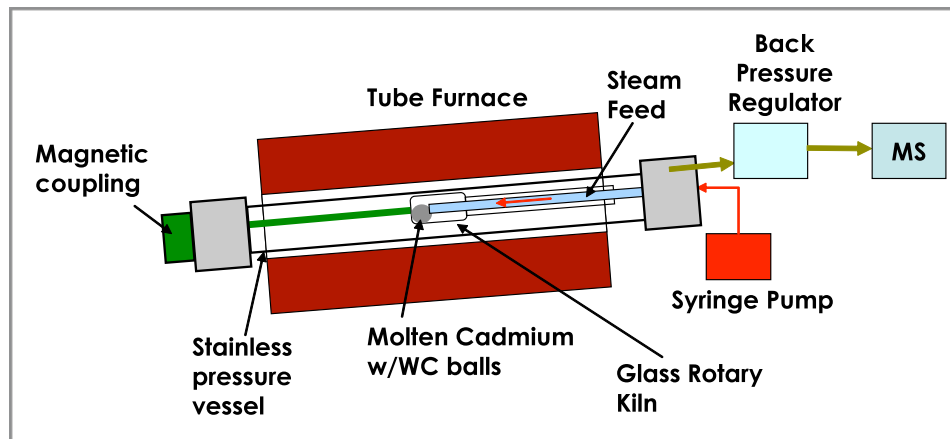


Figure 4.5.3 Conceptual rotating kiln counter flow hydrolysis reactor with tungsten carbide balls to enhance steam/Cd interaction

Operationally, the cycle suffers from the need to manage solids transport along with liquids and gases, but most separations are easy unless an inert gas is used to reduce recombination in the decomposition step. In the case of the hydrolysis reactor, operation at elevated pressure is proposed in response to counter elevated Cd vapor pressure at hydrolysis operating temperature. A high temperature/high pressure separation of hydrogen from steam will be required but design concepts were not available at the time of the evaluation. Alternatively, the steam could be condensed, allowing easy separation of hydrogen, but plant efficiency would diminish significantly. Finally, plant shutdown could raise serious difficulties without incorporation of auxiliary heating to prevent solidification of molten cadmium in vessels and pipes.

Both of the primary chemical reactions have been demonstrated in laboratory studies, but neither has been implemented in operational component designs to allow evaluation of feasibility of closed cycle operation. Data necessary for establishing reaction yields and downstream product concentrations did not exist at the time of the evaluation.

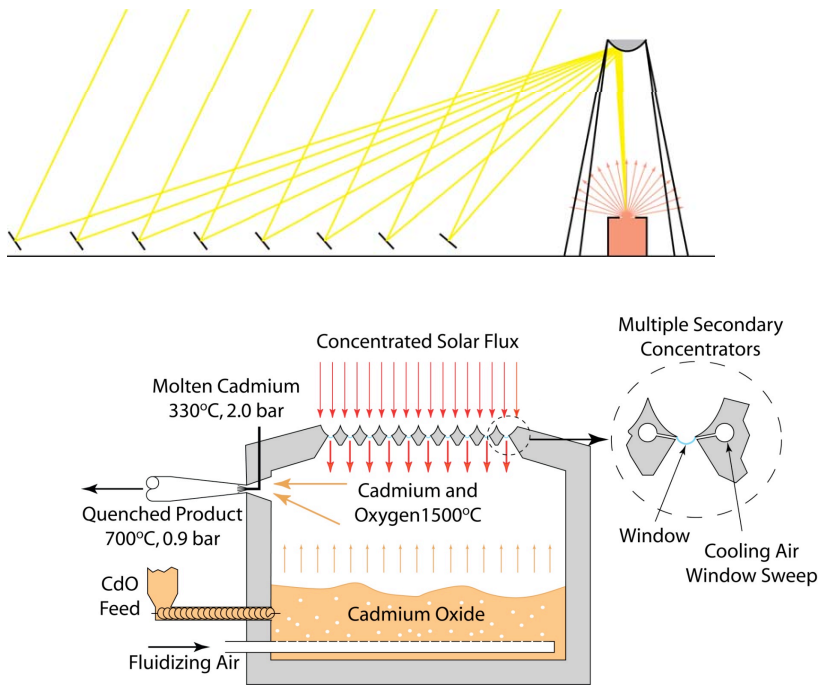


Figure 4.5.4 Beam down collector integrated with fluidized bed decomposition receiver/reactor

Integration with solar power was proposed to be achieved using a “beam down” collector design illuminating a cavity receiver on the ground. (Figure 4.5.4) Preliminary beam down design work performed by the Weizmann Institute called for 10 towers, each surrounded by a graded density nearly circular heliostat field of approximately 700 m diameter providing about 72 MWth to a fluidized bed decomposition receiver/reactor. A beam down solar collector system at the necessary power levels has not been demonstrated. 10 towers with reactor/receivers were required to meet production targets of annual average 100 tonne H₂/day and chemical plants were sized to meet production with two plants serviced by the 10 towers and decomposition reactors.

The proposed molten cadmium quench process has not been demonstrated. Preliminary modeling was underway at the time of the evaluation to allow assessment of the fraction of Cd vapor that would condense on the quench droplets and the rate of condensation removing Cd from participation in gas-phase recombination. Since some recombination will necessarily occur at the vapor-liquid interface, a lower surface/volume ratio of molten Cd will reduce the recombination fraction and increase the Cd metal yield for recycle to the hydrolysis section. On the other hand, longer residence time in the gas phase increases gas-phase recombination and reduces the Cd metal yield for recycling. Rapid quench is desirable, but Cd supersaturation must be kept below the threshold for homogenous nucleation since the surface/volume ratio under

homogeneous nucleation is exceedingly high and Cd metal yield will diminish sharply. Determining molten Cd quench feasibility and optimizing quench conditions was not done at the time of the evaluation.

Table 4.5.1 Advantages and challenges for the Cadmium Oxide cycle

Advantages	Challenges
Simple 2-step process	Cd hazardous material management
Materials abundant and relatively cheap	Molten Cd quench
High thermal efficiency	High temperature/high pressure H ₂ separation
Thermal storage	Solids transport over significant distance
Chemical processes are ground-based	Plant shutdown management

A detailed flow sheet for the CdO cycle was not presented at the evaluation meeting. However, an earlier presentation by the team included a flowsheet that predated the evaluation by about 10 months. That flowsheet is presented here in Figure 4.5.5 with the caveat that it should not be interpreted as reflecting the process at the time of the evaluation.

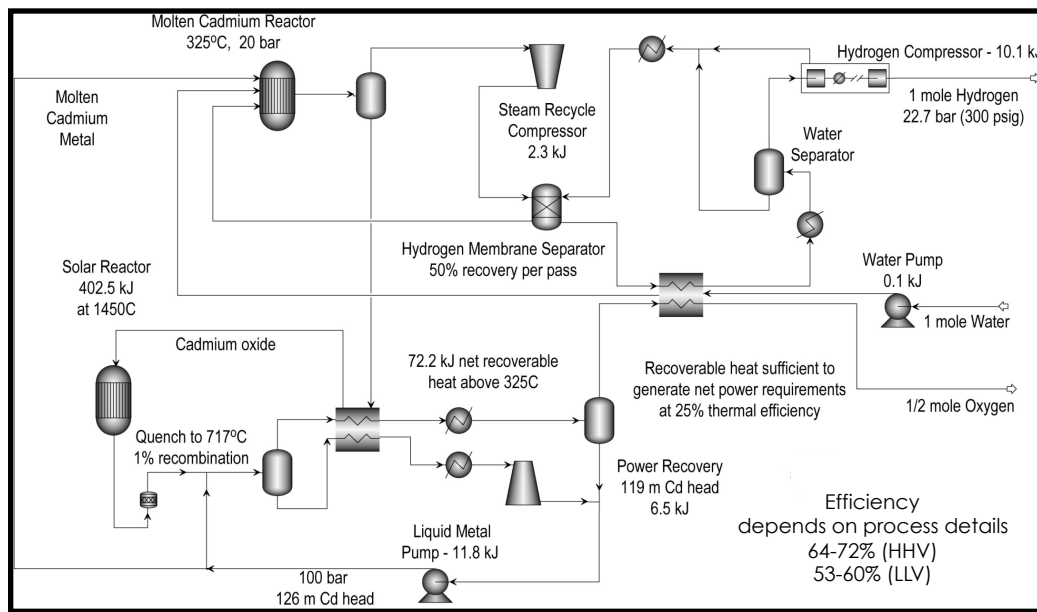


Figure 4.5.5 CdO cycle flowsheet, AIChE Meeting, Salt Lake City, November 7, 2007

Since the process changed significantly after this flowsheet was developed, Aspen Plus™ analysis and optimization will not be addressed. Preliminary H2A analysis for a 2015 case study was presented at the evaluation but documentation was not thorough and the analysis had not been reviewed prior to the evaluation. The cost figures presented at the evaluation are included here for historical purposes and the hydrogen production cost cited by the team is shown but should not be relied upon for comparative purposes.

Table 4.5.2 Component capital costs cited for CdO cycle at the time of the evaluation

Component	Cost
10 beam down solar collector receiver systems	\$352.8 M
10 CdO decomposition reactor vessels	\$72 M
Heat exchangers/hydrolysis reactors	\$33.4 M
H2/H2O membrane separation units	\$8 M
Vertical vessels/separators	\$13 M
Turbines and pumps	\$29.8 M
Solids transport	\$7.7 M
H2 compressors	\$15.5 M
Total Capital	\$532.2 M

Table 4.5.3 CdO operating costs cited at the time of the evaluation

Item	Cost
Electricity	\$0.0682/kW-hr
Purified water	\$0.00132/liter
Cooling water	\$0.0000509/liter

Item	Cost
78 eng/tech staff members	\$6.9 M/yr
Maintenance	\$8.7 M/yr
Total O&M	\$32.8 M/yr

Table 4.5.4 Assumptions for 2015 case study cost analysis

Assumptions	
Startup Year	2015
Hydrogen Production, kg/yr (Peak)	133,333
Capacity Factor	75%
Hydrogen Production, kg/yr (Average)	100,000
Cost of Electricity, \$/kW-hr	0.0682
Cost of Cooling Water, \$/gal	0.000079
Inflation, %/year	1.9
Cost of Heliostats, \$/m ²	\$127

Table 4.5.5 CdO cost estimates with some sensitivity estimates

Results		
Baseline Hydrogen Cost, \$(2005)/kg	\$3.94	
Baseline Hydrogen Cost, \$(2015)/kg	\$4.75	
Sensitivity Factors	Low/High	Hydrogen Cost, \$/kg
Cost of Electricity, \$/kW-hr	0.04/0.097	\$3.92/\$3.95
Capital Cost of Hydrogen Plant	-25%/+50%	\$3.77/\$4.28
Capacity Factor	70%/80%	\$4.21/\$3.69
Cost of Heliostats, \$/m ²	120/160	\$3.86/\$4.31
Hydrogen Plant Efficiency, % (LHV)	40/59.6	\$5.83/\$3.94

Table 4.5.5 presents cost estimates and sensitivity effects for the CdO cycle under the assumptions in table 4.5.4 and using the capital and operating cost estimates shown in tables

4.5.2 and 4.5.3. The H2A analysis was unreviewed at the time of the evaluation and no projected costs for improvements for the 2025 case were presented.

The Cadmium Oxide cycle shows promise primarily through its high thermal efficiency, but overall efficiency could suffer significantly as the challenges listed in Table 4.5.1 are addressed. Whereas cycle simplicity remains a plus, that simplicity is somewhat offset by the volatile and hazardous primary material. The highest priority issue to be resolved is establishing and demonstrating an effective quench process. Without that, everything else is speculative. It was agreed that molten Cd quench feasibility should first be addressed via modeling and simulation before attempting to demonstrate the process in the laboratory. That work was proceeding after the evaluation meeting. Scaled performance modeling of the beam down solar system might have been done, but definitive results and description of the process were not made available. If not done, such modeling is essential to confident estimates of solar system cost

4.6 Sodium Manganese Cycle

The original Sodium Manganese cycle is a non-volatile metal oxide and is attractive both because its thermal efficiency is among the highest of the cycles studied (along with the Cadmium Oxide cycle) and because its reactants are both abundant and nonhazardous. The cycle steps are shown in schematic form in Figure 4.6.1.

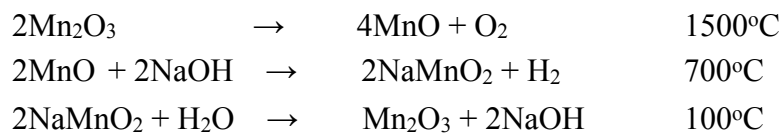


Figure 4.6.1 Schematic steps for the Sodium Manganese cycle

The straightforward cyclic process in Figure 4.6.1 requires considerable excess of water in the hydrolysis step to recover Mn_2O_3 and form aqueous NaOH. The aqueous solution must be concentrated by vaporizing the water to provide NaOH for the hydrogen production step. The excess water removal reduces cycle thermal efficiency so a secondary metal, Zn, was added to improve the hydrolysis step and reduce the required excess water and aid in Na recovery. Figure 4.6.2 shows the operational chemical steps for 3:1 Mn:Zn stoichiometry^{48,50,65,66}.

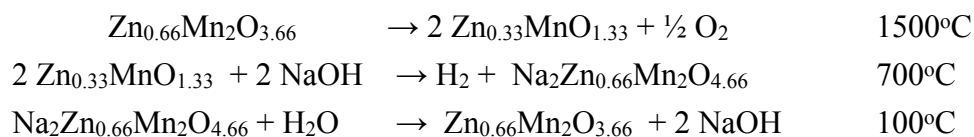


Figure 4.6.2 Mixed metal oxide steps for the Sodium Manganese cycle

Both zinc and iron were tested for hydrolysis improvement and zinc showed significantly better performance, reducing the amount of water required by about a factor of 3. Even so, about 10 moles of water were required for production of 1 mol H₂. The secondary metal appears to prevent, or at least inhibit the formation of a sodium/manganese birnessite that does not participate in the hydrolysis reaction and would be carried through the high temperature step. The consequence of this side reaction is not known. If the birnessite does not decompose, then birnessite would likely accumulate and the reaction could not be closed. If it does decompose, it will likely reduce cycle efficiency, possibly to the point that economics are not competitive. Laboratory experiments demonstrate recovery of only about 80% of the sodium although closed cycle would require recovery of 100% unless the birnessite decomposes in the high temperature step and the sodium is made available once again for hydrolysis. This would change the reaction class from a nonvolatile metal oxide to a mixed volatile/nonvolatile metal oxide since the sodium would vaporize in the high temperature process.

The reduction step was demonstrated in both thermogravimetric analysis and flowing aerosol experiments. The effects of recombination were minimized by reducing oxygen partial pressure with simultaneous inert gas flow so that a closed system design would have to include oxygen/inert gas separation. Conversion efficiency was greater than 80% when a fluidized bed of Mn₂O₃ was reduced to MnO but apparatus design for continuous (as opposed to batch) operation of a fluidized bed was not described. The team noted that residual sodium from incomplete hydrolysis as well as the secondary metal used to reduce the amount of NaOH leach water could undergo volatilization in the reduction chamber with consequent loss through wall condensation and possible corrosion consequences. These obstacles were not evaluated in the experiments and not addressed in the system model used for analysis.

Release of hydrogen by mixing MnO with NaOH at ~700°C is complicated by the mixing of liquid NaOH with solid MnO and Zn-Mn-O compounds. Nearly 100% reaction has been reported for NaOH and pure MnO but those earlier results could not be repeated with the mixed metal oxide used for improved sodium recovery. Some evidence was found that indicated that NaOH was vaporized and lost to the reaction. No such effect was observed for the pure MnO/NaOH reaction. The team speculated that sodium and oxygen could be trapped in the MnO structure but it remains unclear why this would occur in the mixed metal oxide process and not in the pure MnO process. Many issues remain unresolved for the hydrogen release process so that closed cycle feasibility remains uncertain

Table 4.6.1 Advantages and challenges for Mx-Sodium Manganese

Advantages	Challenges
High thermodynamic efficiency	Excessive leach water for Na recovery
Materials are abundant and non-toxic	Hydrolysis side reactions inhibit closure
Alumina useable in high temperature step	Possible Na volatility: loss and corrosion
Back reaction repressed by reactant state	Low pressure H ₂ formation at 0.1 atm

Figure 4.6.3 shows the process flowsheet used for cost and performance analysis of a 3:1 Zn:Mn oxide process. The analysis assumed that no Zn or Na was lost due to volatility. The reduction step was assumed to be 80% efficient, the hydrolysis step was assumed to be 100% efficient and NaOH recovery was assumed to be 80% efficient. The analysis assumes cyclic processing for all materials so that no side reactions at to accumulate passive materials from cycle to cycle.

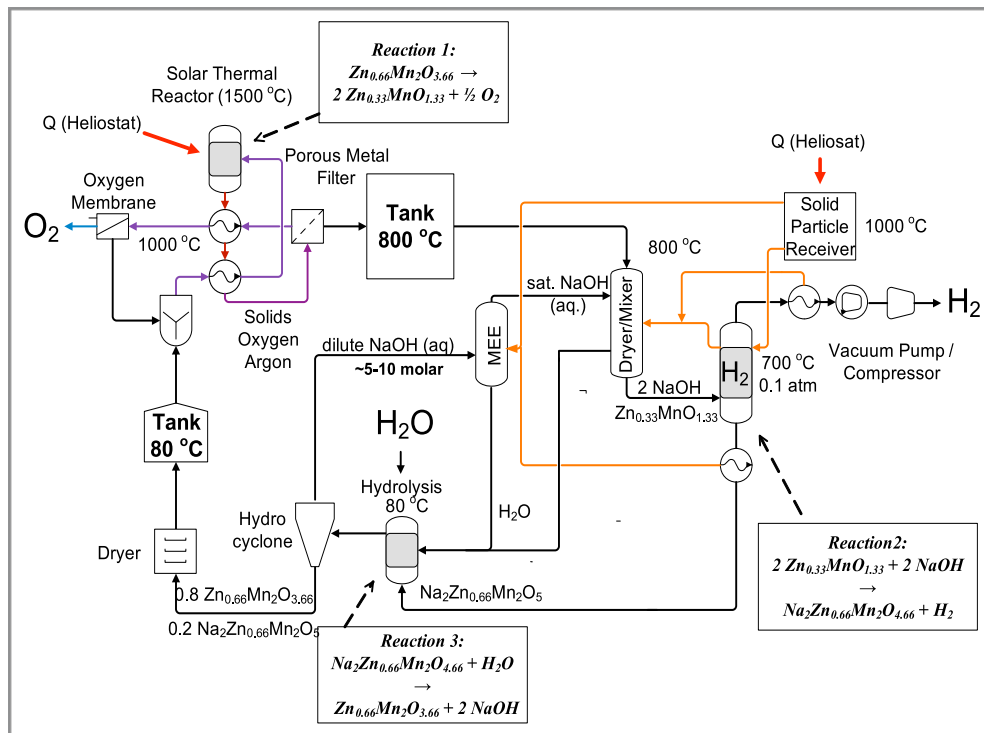


Figure 4.6.3 Schematic flowsheet for analysis of the Mx-Sodium Manganese cycle

Description of the process that follows is liberally extracted from the submitted white paper. The Mn₂O₃ high temperature reaction is carried out at 1500 °C in aerosol flow reactors mounted on six towers. The Mn₂O₃/NaMnO₂/ZnO precursor is transported from a storage tank with a pneumatic transport system to an aerosol feeder system after passing through a heat exchanger to

recover sensible heat from the reaction product. The feeder disperses the powder in a preheated inert argon stream to further minimize the thermal load of the reactor prior to entering the solar furnace. The effluent of the reactor is rapidly quenched to 800 °C with a cool argon/oxide feed stream to minimize recombination of the reduced metal oxide and oxygen. The cooled aerosol stream passes through a metal filter at ~800 °C that removes the solid reaction product from the oxygen containing argon stream for storage and further processing. The argon/oxygen stream is heated to ~1000 °C and passes through a membrane module equipped with a ceramic oxygen transport membrane. The purified argon is then recycled into the process.

The reduced oxides produced during the daytime operation of the high temperature reduction (formally a mixture of MnO/Mn₂O₃/NaMnO₂/ZnO) are stored at 800 °C in insulated tanks for 24/7 production of hydrogen. The powders are mixed with a concentrated solution of NaOH. The residual water is vaporized in a dryer and the heat of vaporization is supplied by the latent heat of the hot oxides. The solid NaOH/oxide mixture is then reheated in a furnace to >650 °C to form hydrogen. It is assumed that the process is carried out continuously but the need for 0.1 atm vacuum might require several smaller batch reactors.

The product from the hydrogen reaction (formally NaMnO₂/ZnO/Mn₂O₃) is hydrolyzed with excess water at 80-100 °C. The hydrolysis product is a mixture of solid oxides and an aqueous NaOH solution. A multi-effect evaporator system concentrates the NaOH solution that is about 5-10 molar to saturation (~25 molar) for recycling into the hydrogen formation reaction. The water is recovered as a liquid to be recycled into the hydrolysis reaction.

The energy required for the high temperature on-sun reaction is supplied to eight 221 m high towers that are irradiated by 24 heliostat fields with 934 heliostats each (111 m²/heliostat) for a total area of 2.5x10⁶ m².

The supplemental energy required for hydrogen formation and to recycle NaOH after hydrolysis is obtained from a solid particle receiver/sand storage system. The particle receivers are mounted on three 181 m high towers and utilize an inorganic storage material that is heated to 1000 °C during daylight operation. The heat is supplied by 12 heliostat fields with 934 heliostats each (90 m²/heliostat) for a total heliostat area of 1.03 million m². The heated sand is stored in holding tanks for the 24/7 low temperature hydrogen formation and sodium recovery steps. The thermal efficiency for the HHV of H₂ based on the energy delivered to the reactor is estimated to >45%. This calculation may be optimistic since heat losses during transport and storage of the hot materials are not accounted for. Figure 4.6.4 shows schematically the proposed plant layout

with a single chemical plant serviced by 8 high temperature towers and 3 moderate temperature solid particle receivers

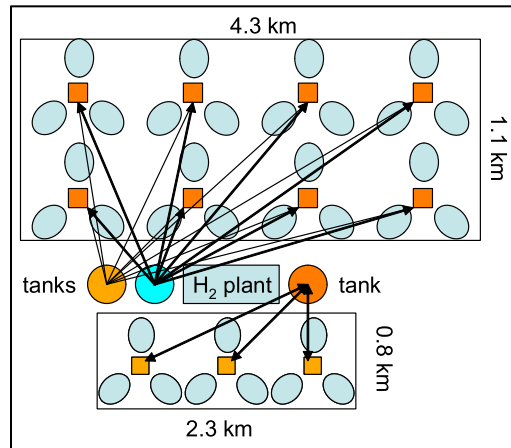


Figure 4.6.4 System layout with a single chemical plant for the Mx-Sodium Manganese cycle

H2A analysis was presented but details were provided only for a 2015 case study even though estimated product costs were given for both 2015 and 2025. The documented difference between the 2015 and 2025 case studies was heliostat cost of \$126.50/m² in 2015 and \$90/m² in 2025. Significant uncertainty in process cost persisted largely because assessment of side reaction effects remained to be done and, for example, evaluation of possible recuperation of energy from the rapid quench process. Uncertainties in component costs were cited and these appeared sufficiently significant that listing estimates for these costs would be pointless. These uncertainties are shown in Table 4.6.2.

Table 4.6.2 Component uncertainties for the Mx-Sodium Manganese cycle

Component	Issue
Ar/O ₂ separation	VSA too expensive; membrane does not exist
SPR heat exchangers	Not designed/tested
Solids transport	Not designed/tested
Hot storage for oxide	Not designed/tested
Hot storage for sand	Not designed/tested

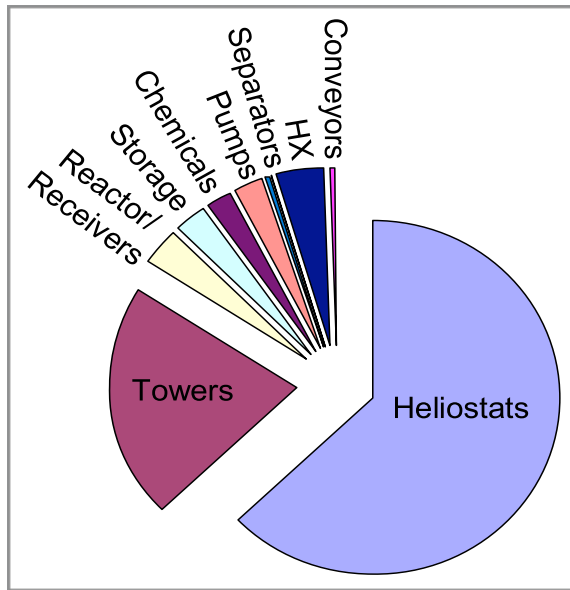


Figure 4.6.5 Estimated capital cost distribution for the mixed metal oxide realization of the Sodium Manganese cycle

Figure 4.6.5 shows the estimated installed capital cost allocation for 2015 of \$668 M. No similar figures were available for the 2025 case study although H₂ gate costs were estimated for 2015 - \$5.22/kg H₂ - and for 2025 - \$4.22/kg H₂.

The R&D team concluded that resolution of the remaining issues for this cycle would be unlikely to reduce the product cost sufficiently to meet the program cost targets and recommended that further work on the cycle be terminated. A *sine qua non* for this cycle is discovery of a means of sodium recovery without inordinate water addition that does not excite side reactions so that cycle closure is assured.

4.7 Sodium Manganate

The failure of the standard Sodium Manganese cycle suggested a modification of the process whereby sodium would be re-circulated to the high temperature reaction. TGA measurements at 1500°C confirmed that the reduction of NaMnO₂ to pure MnO and vapor phase Na_xO_y proceeds slowly to completion. The reaction will be feasible if it can be confirmed that the complete vaporization of Na is not necessary for the reduction of Mn(III) to Mn(II) or that the reaction proceeds sufficiently fast in an aerosol with small particle sizes. Vaporized sodium compounds will likely re-condense on the MnO particles as the product mix is cooled to lower temperature since the particles will provide a large number of nucleation sites. Thermodynamic predictions indicate that sodium will be recovered after the reaction in the form of either Na metal, Na₂O, or

Na_2O_2 . Any of these species will easily hydrolyze to NaOH in the presence of liquid water or steam which then can be reduced with MnO to hydrogen and NaMnO_2 at temperatures above 650°C similar to the original manganese cycle. In addition, the high affinity of sodium for oxygen might minimize recombination with Mn since gas phase oxygen will more likely react with vaporized sodium and form one of the oxide species. A fluid wall reactor for the high temperature step might be necessary to prevent deposition of sodium compounds. The cycle is shown in more detail in Figure 4.7.1.

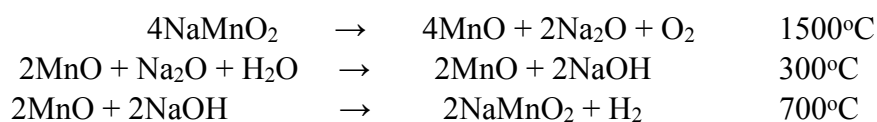


Figure 4.7.1 Reaction path for the preliminary Sodium Manganate cycle

A preliminary H2A estimate suggests that this cycle might yield H_2 costs in the range of \$3/kg since the large excess energy requirements for sodium recovery as well as the additional sensible heat for the inert component in the mixed oxide cycle are avoided. In addition, both reaction steps are endothermic and therefore, the need for heat integration is minimized.

At the time of the evaluation, insufficient work had been performed on this concept to warrant further details in this report. What work had been done found that the reduction step was slow and the team was directed to focus its study on kinetics of the reduction. Additional work would be required to assess the role of vapor phase Na and its corrosion effects on container materials.

4.8 ALD Ferrite

Ferrite material used as a water oxidation/reduction agent to generate hydrogen from water has been under study for a number of years^{55,58}. Virtually all ferrite materials produced as co-precipitates have suffered from very similar drawbacks. Conversion efficiency is low for the reduction step, oxidation using water is slow and the active material performance degrades under cyclic operation. Most previous ferrite work studied co-precipitated ferrite material from solution onto (and sometimes into) a substrate. The resulting active material is essentially heterogenous in distribution and composition and characteristics continue to change under the severe cyclic thermal environments. The chemistry is schematically shown in Figure 4.8.1.

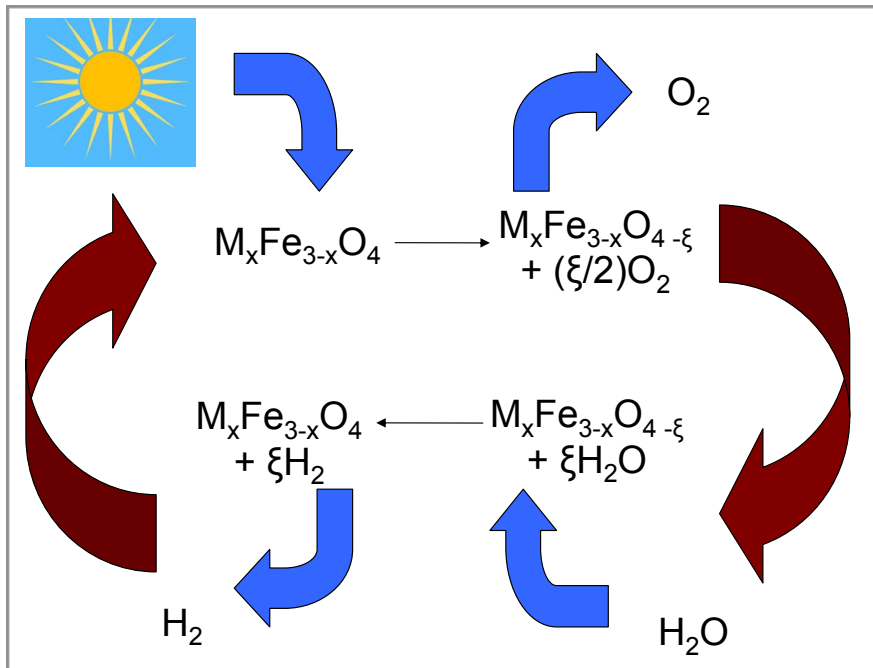


Figure 4.8.1 Schematic chemistry of a water-splitting ferrite cycle

Applying methods of Atomic Layer Deposition (ALD), it is possible uniformly to deposit virtually identical layers of material interspersed with other material itself uniformly deposited in virtually identical layers. Using this technique, a highly uniform and thin layer of $CoFe_2O_4$ can be established on a substrate as illustrated in Figure 4.8.2. Alternating layers of CoO and Fe_2O_3 are deposited using ALD and then the layers and substrate are calcined resulting in a highly uniform and thin layer of cobalt ferrite. Heating the layer to between $1200^{\circ}C$ and $1500^{\circ}C$ gives rise to thermal reduction with the cobalt ferrite converting possibly to an alloy of CoO and $2FeO$ and release of oxygen. Exposure of the alloy to steam at a temperature of about $1000^{\circ}C$ releases hydrogen and restores the original composition of the layer. X-ray dispersive (XRD) analysis of the ALD layer showed no crystallinity change after thermal reduction. No data was shown for layer characteristics after water oxidation.

Preliminary experiments showed that the ALD ferrite (Fe_3O_4) reacted much more quickly than the co-precipitated cobalt ferrite ($CoFe_2O_3$) but the cobalt ferrite provided measurably higher conversion efficiency. In another experiment, co-precipitated cobalt ferrite was compared with ALD cobalt ferrite. Here, the ALD sample showed both faster response and higher conversion efficiency than the co-precipitated sample.

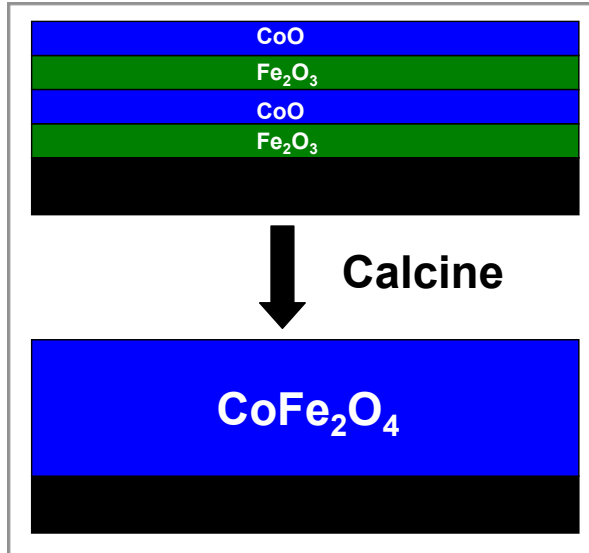


Figure 4.8.2 ALD deposition of uniform thin layer of cobalt ferrite

Another set of experiments examined the effect of substrate by comparing ALD cobalt ferrite performance when deposited on zirconia and on alumina. A number of observations are noteworthy. First, thermal reduction of cobalt ferrite on alumina substrate initiates at much lower temperature (~900°C) than for zirconia substrate (~1200°C). Second, since the response time is roughly the same for both substrates, the conversion efficiency is higher for alumina than for zirconia. The third observation is that cobalt ferrite reduction on alumina forms hercynite (FeAl₂O₄) which appears to persist from cycle to cycle. Finally, response times and conversion efficiency for the hercynite material appear to be stable over multiple cycles.

These promising observations provided basis for recommending that ALD ferrite materials continue under investigation even though none of the requirements for the evaluation process had been met. The primary uncertainty for ALD ferrite systems was determined to be its physical durability and chemical stability under repetitive thermochemical cycling and this feature was called out as the critical path item for focused study. In spite of this recommendation, a great deal of work remains to be done before this cycle could assume serious competitive stature. Cycle thermodynamic performance needs to be quantified and its potential thermal efficiency evaluated. An operational concept needs to be developed that shows consistency with whatever form of active material is selected for cycling. Given that form, the conversion efficiency and kinetics (or residence time) need to be quantified and a means of heat recuperation must be identified and designed in order to maintain an acceptable level of cycle thermal efficiency. Moreover, since the active material is fabricated, the cost of material and fabrication must be established. Satisfaction of these requirements should permit assessment of

capital and operational costs from which to estimate product cost in a way consistent with the assumptions and guidelines imposed on the other thermochemical cycles.

4.9 Hybrid Copper Chloride

The Hybrid Copper Chloride cycle is a 3-step process requiring relatively low temperature but also requiring an electrolysis step to release hydrogen and convert CuCl to the original CuCl_2 for the hydrolysis reaction. Research and development of this cycle is relatively mature with all reactions verified in the laboratory but discovery of a durable membrane and electrolysis conditions preventing copper crossover had not been achieved at the time of the evaluation^{60,76,77,78,79}. The process is described by hydrolysis of CuCl_2 to form copper oxychloride (Cu_2OCl_2) and HCl . Cu_2OCl_2 is decomposed in the high temperature step to form CuCl and release oxygen. The CuCl and HCl are electrolyzed to release hydrogen and form CuCl_2 . Figure 4.9.1 shows the hybrid thermochemical process.

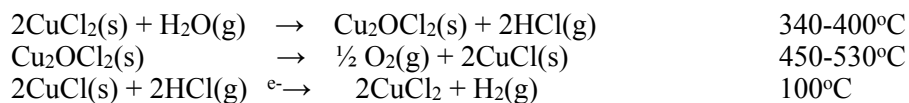


Figure 4.9.1 Hybrid Copper Chloride chemistry

The Hybrid Copper Chloride team includes Argonne National Laboratory (ANL), Atomic Energy of Canada, Ltd., Pennsylvania State University, the University of South Carolina, Tulane University, and the universities associated with the Ontario Research Foundation. The team reflected a relatively loose federation except for Pennsylvania State University and the University of South Carolina which ultimately executed subcontracts with Argonne to undertake specific tasks in support of the Argonne project.

Laboratory work demonstrated proof of concepts assuring cycle closure. Chlorine gas was thought to be a possible side reaction product of Cu_2OCl_2 decomposition but experiments at NREL and CEA showed no Cl_2 presence. Further experiments must be done to resolve the contrast between the ANL, NREL and CEA results but this side reaction is not expected to be an issue. Reaction yields were good for the hydrolysis and decomposition tests and reactor designs have been developed but not fully fabricated and tested. A decomposition temperature of 550°C gave 100% O_2 recovery in laboratory testing. This result suggests complete reaction of the decomposition step in light of the NREL and CEA negative tests for chlorine gas. Indirect evidence for performance of the hydrolysis reaction rests on heat and mass transfer measurements using an ultrasonic nebulizer.

Table 4.9.1 lists advantages and challenges for the Hybrid Copper Chloride cycle as interpreted by the R&D team.

Table 4.9.1 Advantages and challenges for Hy-CuCL

Advantages	Challenges
Lowest high temperature for STCH	Copper crossover in electrolyzer
System efficiency meets target	500 mA/cm ² at 0.63 V
Active materials cheap and abundant	Separation of spent anolyte
Cycle has long history of development	Excess water or low pressure for hydrolysis
Chemistry components commercially used	Possible Cl ₂ gas from decomposition step
Materials of construction identified	Amount and effect of carryover reagents
	Chemistry and system modeling difficult

Cycle efficiency and product cost parameters are sensitive to the electrolyzer performance for the targeted current density of 500 mA/cm². Table 4.9.2 shows this dependence for the system design concept at the time of the evaluation. Whereas demonstrated electrolyzer performance at the time of the evaluation was 429 mA/cm² at 0.9 V, there are engineering solutions that should

Table 4.9.2 Hy-CuCl system performance sensitivity to electrolyzer performance

Cell emf at 500 mA/cm ²	System efficiency (LHV)	Product cost (\$/kg H ₂)
0.7 V	39%	4.53
0.63V	41%	3.48

improve the performance like higher operating temperature and electrolyte stirring. Nevertheless, engineering solutions will not supplant the need to discover a membrane material and operating conditions that prevent copper crossover and cathode deposition since initial performance will degrade by such behavior.

Figure 4.9.2 shows a conceptual block flow chart for the process and is useful in discussing cycle challenges. Technical issues for the electrolyzer cell were discussed above. Chemical and

materials challenges remain in the crystallizer and hydrolysis sections. For example, it is not practical to maintain a continuous flow process and drive the electrolysis reaction to completion. That means that an aqueous mixture of CuCl_2 and CuCl will flow as spent anolyte to the crystallizer. CuCl must be separated and recycled to the electrolyzer as complement to fresh anolyte while the CuCl_2 is directed to the hydrolysis reactor to form copper oxychloride for feed to the high temperature decomposition reactor. Spent anolyte separation has not been demonstrated although membrane distillation or electrodialysis have been identified as possible methods.

Reactor components suitable for testing and scale-up have not been fabricated and tested and materials of construction have not been selected although glass-lined components are mentioned as routine for other applications with similar reagents. The amounts and effects of recycled reagents have not been demonstrated.

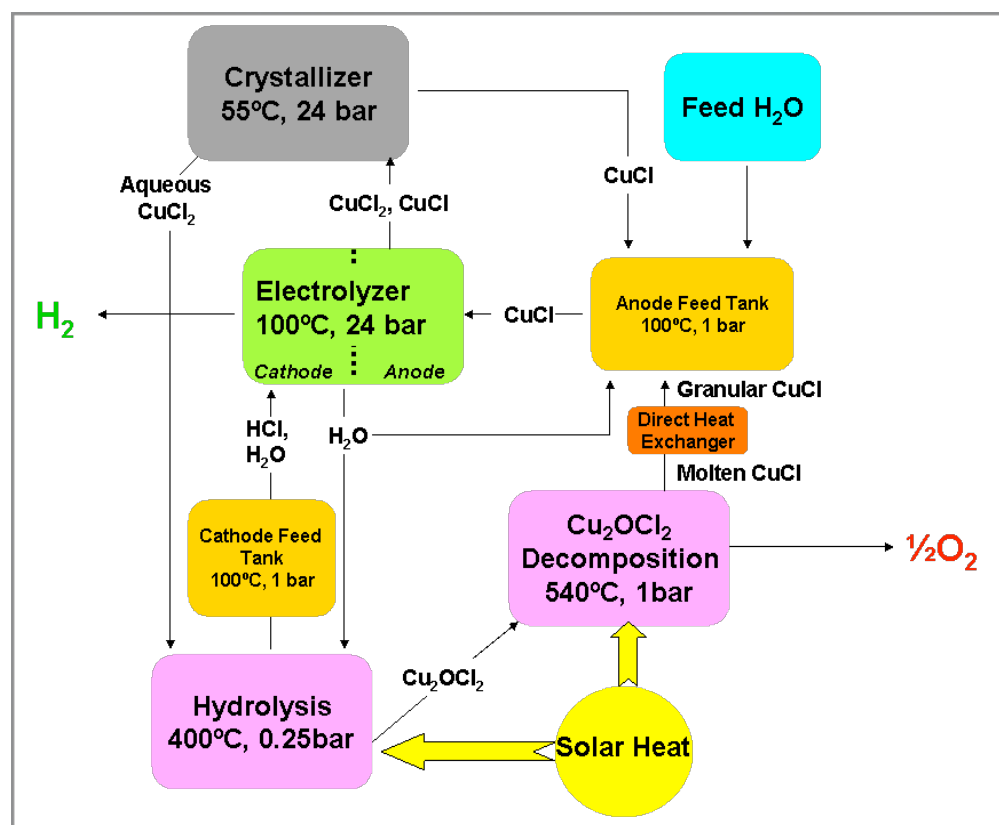


Figure 4.9.2 Hy-CuCl conceptual block flow chart

A detailed flowsheet was not presented for the evaluation, but AspenPlus™ analysis has been underway for some time. Inadequate data and the complexity of the process prevented

convergent optimization at the time of the evaluation. The solar collector/receiver concept was not described, reportedly because of teaming with a commercial collaborator whose information was proprietary. Nevertheless, H2A analysis was shown in the presentation and is repeated here.

Table 4.9.3 H2A analysis results for Hy-CuCL

Case	Solar/Chemical Capital (\$M)	Cell EMF V	Elect Cost \$/kW-hr	Product cost \$/kg H2	Sensitivity	Efficiency % (LHV)
2015	208.3/136	0.7	0.068	4.53	3.78-5.31	39
2025	168.5-106.6	0.63	0.048	3.48	2.91-4.11	41

Capital cost reductions in this unreviewed H2A analysis were due to

- Heliostat cost reduction from \$127/m² to \$90/m² (~\$40M savings)
- Reduced hydrolysis reactor residence time
- Reduced decomposition reactor size (~\$30M savings)
- Reduced electrolyzer costs by use of Pd instead of Pt, increased efficiency and durability (~\$2M savings)

The path forward for Hy-CuCl is critically dependent on discovery of materials and operating procedures that permit durable electrolyzer performance at ~500 mA/cm² and ~0.63 V without copper crossover and cathode deposition. This feature of R&D must be achieved in order for the cycle to meet efficiency and product cost targets.

Additional development is necessary to manage hydrolysis reactor performance. Presently, either excess water or low pressure reactor operation is required to achieve satisfactory hydrolysis yield of copper oxychloride. The first option entails water removal from the product stream and the second requires compression work. The tradeoff between these two options is not clear, nor is it evident that consideration has been given to other hydrolysis processes like a mix of excess water and lower pressure operation. Detailed Cu₂OCl₂ decomposition testing is necessary to resolve fully the issue of chlorine gas release. Recovery of released chlorine is possible but would add to the complexity and cost of the system. Corrosive activity of molten CuCl needs to be determined to permit optimal selection of construction materials. Finally, considerable laboratory work is needed to acquire necessary data to support component modeling and AspenPlusTM analysis.

5. Summary Remarks and Recommendations

5.1 General Observations

The selection of projects for termination engages the problem of deciding when future benefit is not balanced by earlier investment and necessary resources for continuation. The process is facilitated by the identification of quantitative performance metrics and, at the same time, made difficult by the assessment of work still in progress so that performance is projected and not assured. No easy solution to this conundrum exists because investment expense necessary to assure performance prediction usually exceeds what is available and/or reasonable. A competitive process, pitting one idea against another, can be used to make decisions for work-in-progress, but relies on judgement calls that might not always reflect the most appropriate technical expertise and that could reflect interest conflicts if judgement sources are not carefully chosen.

The competitive process is further complicated by contrast in project maturity. It is self-evident why middle-school players are not fielded against university-level players and roughly the same rationale applies to projects in widely different stages of R&D. It is difficult to make comparative assessments of potential when some teams have had significantly more opportunity than others to survey options, perform tests and make “path-forward” decisions.

All of these issues would be irrelevant if one or more cycles showed clear dominance in terms of meeting the established quantitative performance metrics. However, none of the STCH projects could clearly and definitively demonstrate performance in line with the DOE targets. In fact, it is rather surprising that projected performance metrics generally were close to the targets, but still outside desired levels. It is possible that cycles selected for investigation reflect “best of show” and that thermochemical processes are simply unable to meet target performance metrics. It is also possible that more R&D is needed to establish better cost and performance projections.

None of the evaluated cycles projected performance consistent with DOE targets. Moreover, there was no cycle under consideration whose inferred potential warranted certain favor over all the other cycles. R&D maturity of cycles under evaluation showed remarkable range with several cycles having experienced about a year of development effort while several others had development history that exceeded 30 years (not all of which reflected active R&D). Finally every cycle under consideration reported technical obstacles whose resolution was essential to serious consideration for development to pilot plant design. These four features of the cycles under evaluation led to the conclusion that no substantive decision could be made to terminate

R&D of any specific cycle unless the cycle proponent declared that targets could not be achieved in the absence of progress that in the proponent's opinion was unlikely.

The evaluation and selection effort was conceived to facilitate focus of available resources on continued development and realization of cycles most likely to transition from R&D through pilot plant to commercial deployment. The absence of discriminating features adequate to focus resources on a few cycles led to an outcome that was different from intended but arguably as useful. The existence for all cycles of performance-critical obstacles permitted focus of resources on resolution of those obstacles and successful prosecution of such resolution would be necessary for R&D continuation.

5.2 Evaluation Outcomes

The following summarizes R&D priority on critical path obstacles derived from the evaluation process for each cycle under consideration. Successful resolution of critical path items does not assure cycle success, but failure to resolve critical path obstacles assures the cycle cannot be competitive. For those cycles whose R&D was terminated by recommendation of the cycle proponent, necessary progress is described in those areas that could lead to its restoration to active R&D status.

5.2.1 Sulfur Iodine

R&D for this cycle is under management by the Office of Nuclear Energy. Critical path obstacles are not subject to mandate by the Office of Energy Efficiency and Renewable Energy. Consequently, the critical path obstacle is an observation, not a direction. Findings are:

- Hydrolysis (Bunsen) reaction unreliable and may not go to completion
- Hydriotic acid decomposition step not demonstrated adequately to support system analysis
- Amount and effects of carryover reagents unknown
- Sulfuric acid decomposition reactor component lifetimes unknown
- Solar thermal integration not designed or tested

The STCH critical path obstacle for the Sulfur Iodine cycle was identified to be solar thermal integration with the Solid Particle Receiver (SPR). Resolution of this obstacle is complicated by absence of STCH funding for SPR development, but includes:

- Identify and test SPR thermal medium verifying durability and absence of sintering⁷³
- Design and test heat exchangers for thermal coupling of SPR to thermochemical process
- Design and test scaleable SPR

5.2.2 Hybrid Sulfur

R&D for this cycle is under management by the Office of Nuclear Energy. Critical path obstacles are not subject to mandate by the Office of Energy Efficiency and Renewable Energy. Consequently, the critical path obstacle is an observation, not a direction. Findings are:

- Electrolyzer membrane performance limited by sulfur crossover and deposition
- Sulfuric acid decomposition reactor component lifetimes unknown
- Solar thermal integration not designed or tested

The STCH critical path obstacle for the Hybrid Sulfur cycle was identified to be solar thermal integration with the Solid Particle Receiver (SPR). Resolution of this obstacle is complicated by absence of STCH funding for SPR development.

- Identify and test SPR thermal medium verifying durability and absence of sintering⁷³
- Design and test heat exchangers for thermal coupling of SPR to thermochemical process
- Design and test scaleable SPR

5.2.3 Photolytic Sulfur Ammonia

R&D for this cycle was in a very early stage at the time of the evaluation, having been active for less than a year. Nevertheless, the rationale for this cycle was founded on more efficient use of solar radiation by spectral beam splitting and distribution of spectral components to photoactive and thermal steps. The R&D team proposed either spectral beam splitting using a single solar field or using dual solar fields with one dedicated to the photoactive process and the other dedicated to thermal processes. It is argued that the dual field approach does not use solar radiation more efficiently but the team was directed to evaluate cost and effectiveness of both the dual field approach and the beam splitting approach to resolve general concept design issues before proceeding. Evident skepticism during the meeting resulted in an additional recommendation to evaluate the feasibility and value of replacing the photolysis step with an electrolysis process.

5.2.4 Zinc Oxide

The Zinc Oxide cycle was thoroughly studied and the proponent recommended termination largely because no path appeared to be feasible that would bring product costs in line with targets. Findings are:

- discovery of reactor materials capable of withstanding thermal shock and operating durably in the necessarily extreme temperature environment and in the presence of oxygen is problematic

- experiments were unable to demonstrate more than 18% zinc recovery in quench of the reduction step because of recombination and projected product costs significantly exceeded target levels even assuming 85% zinc recovery
 - feeding relatively large zinc particles in the quench stream would reduce recombination losses by unknown amount but would generate larger particles for feed to hydrolysis and hydrolysis efficiency would suffer
 - use of a high temperature oxygen transport membrane or flowing inert gas with the quench stream could reduce recombination but both approaches would entail a high temperature gas separation that was not designed
- loss of zinc to reactor walls might be avoided by use of a fluid wall design but would entail a gas separation process

A means of recovering at least 70% zinc metal while retaining hydrolysis efficiency would be necessary to warrant investment in materials discovery for fabrication of an effective reduction reactor and continued cycle development.

5.2.5 Cadmium Oxide

The Cadmium Oxide cycle has very high thermal efficiency but entails use of volatile hazardous material and the team concluded the thermochemical processing would be safer if performed at ground level instead of on a tower. A beam down receiver/reactor was selected for this purpose. It was not made clear that such a system has ever been tested at the necessary power levels and the solar field capital costs were not made clear during the evaluation. Initial laboratory measurements found that molten cadmium hydrolysis proceeded very slowly and excessive residence time in the hydrolysis reactor was needed to obtain satisfactory CdO yield. However, an effective design that was tested at laboratory scale appeared to resolve the slow kinetics and surface passivation found in the hydrolysis step. TGA measurements confirmed that recombination in the thermal reduction step would need to be mitigated and avoidance of excessive recombination was identified as a critical path issue requiring resolution. The team proposed a rapid quench assisted by inclusion of finely dispersed molten cadmium to promote condensation without initiating homogeneous nucleation that would cause excessive recombination in a rapid quench of pure Cd vapor. The exact details of this quench process require careful analysis of quench droplet temperature, size and number density effects on the rate of Cd vapor condensation in order to assure absence of homogeneous nucleation and to estimate the recovery efficiency of recycled cadmium metal. Modeling a molten cadmium quench process was identified as the top priority effort for this cycle. The team was encouraged to continue working with the Weizmann Institute in Israel to establish firm design and cost of the beam down solar system.

5.2.6 Sodium Manganese

Sodium Manganese shows very high thermal efficiency and uses abundant and cheap reagent materials. The high temperature reduction step is amenable to operation in standard materials like alumina and the reduction back reaction is suppressed in this nonvolatile process. The first obstacle encountered was the need for excess water in the hydrolysis step to permit leach recovery of NaOH. Managing excess water increases product cost so a mixed metal oxide process with zinc was used to reduce water molality. Even so, water molality remained high although about a factor of 3 less than with the pure Mn₂O₂ and experiments were able to demonstrate only about 80% NaOH recovery. It is speculated that some of the sodium might volatilize and be condensed on reactor walls (indeed some evidence of this was found). It is also thought that sodium ions and oxygen might be incorporated in the manganese oxide matrix. Whatever the cause, recovery of NaOH is essential to cycle closure and the team was unable to identify an effective process. The R&D team recommended termination of the mixed metal Sodium Manganese cycle in favor of exploring a sodium manganate thermal cycle. Restoration of the mixed metal Sodium Manganese cycle to active R&D status would require the discovery of a means of sodium recovery without the need for excess water and unaccompanied by side reactions that could remove Na from the active cycle.

5.2.7 Sodium Manganate

This cycle was conceived upon perceptible failure of the mixed metal Sodium Manganese cycle and appeared attractive because sodium would be recycled to the high temperature step as a mixed oxide of Na_xO_y which is easily hydrolyzed to NaOH closing the cycle. In effect, the hydrolysis and oxidation steps do not have to go to completion in order to close the cycle. Since sodium is cheap and abundant, an excess of sodium required by incomplete reactions is of no consequence to cycle economics. Appearance of this concept so late in the project prevented performance of significant work to define and resolve obstacles. However, assuming no irreconcilable obstacles, product cost estimates fell within the DOE targets. One observation is that the reduction step proceeds slowly but completely at about 1500°C but it was not confirmed if the Na_xO_y would have to be vaporized to complete the conversion of Mn(III) to Mn(II). So volatilization and possible corrosion and/or loss to reactor walls remain issues for closure of this cycle. Because the reduction step that was tested in a TGA is slow, it is possible that residence times in the high temperature reduction reactor would not be conducive to operation as a continuous flow aerosol process. Whereas a fluidized bed approach could manage residence time, a continuous process design (as opposed to batch processing) had not been developed at the

time of the evaluation. The R&D team was directed to focus its attention on kinetics of the reduction reaction to determine the feasibility of a continuously flowing aerosol process.

5.2.8 ALD Ferrite

ALD Ferrite is another cycle whose investigation began only shortly before the evaluation. Primary findings of the early investigations were that ALD cobalt ferrite mixtures were both more efficient and faster responding than co-precipitated samples of the same materials. When ALD ferrite is reduced on alumina, hercynite (FeAl_2O_4) is formed and this material showed onset of reduction at much lower temperature (900°C) than ALD ferrite reduced on zirconia (1200°C). Because response times are about the same for both substrate materials, it was concluded that the reduction efficiency of hercynite is higher than that of ALD ferrite and both perform better than co-precipitated ferrite materials. Finally, some cycling experiments were performed that appeared to show physical and chemical material stability. All other ferrite materials tested have consistently degraded in both form and activity so this fact, if borne out by further study, would be a breakthrough in non-volatile metal oxide cycle performance. The ALD Ferrite team was directed to focus effort on establishing the veracity of hercynite stability under repetitive thermochemical cycling. At the same time, the behavior of thin films or small particles would need to be assessed in order to arrive at a conceptual design for a hydrogen production system, but this was not included in the priority task assigned to this cycle. Given active material stability, conversion efficiency and kinetics (or residence time) still need to be quantified and a means of heat recuperation would need to be identified to maintain an acceptable level of cycle thermal efficiency.

5.2.9 Hybrid Copper Chloride

Hy-CuCl is a high thermal efficiency cycle whose thermal reduction temperature is the lowest of all the STCH cycles under active investigation. This is a three-step cycle that requires electrolysis to release hydrogen and close the cycle. Hy-CuCl has been under study by various institutions since the 1970's although R&D experienced a lengthy hiatus before serious work resumed in the early 2000's. Active materials in the cycle are cheap and abundant, the reactor components are similar to others used in common commercial applications and materials of construction have been identified but not optimized. Three difficult obstacles remain to be resolved. First, the use of excess hydrolyzer water can be mitigated by low pressure operation of the reactor, but both options require process energy to manage. Second, spent anolyte containing an aqueous mixture of CuCl and CuCl_2 must be processed to separate these species to direct the CuCl back through the electrolysis step and to direct the CuCl_2 through the crystallizer to the hydrolysis reactor. Several separation options have been identified, but none tested. Finally,

electrolyzer membranes at the time of the evaluation showed copper crossover to the cathode where deposited metallic copper degrades the electrolyzer performance. Competitive performance of his cycle requires electrolyzer current density of about 500 mA/cm² with cell emf of about 0.63 V. The best performance at the time of the evaluation was about 429 mA/cm² at about 0.9 V and the design experienced copper crossover. Whereas engineering solutions for higher current density at lower bias were proposed, the overwhelming obstacle for this cycle remains the discovery of electrolyzer membrane material and associated electrolysis processes that prevent copper crossover. This priority task was defined for the Hy-CuCl team.

5.3 Recommendations

5.3.1 Project planning

The determination to reduce the number of cycles under investigation was and is an appropriate exercise. That this first effort appears to have been premature does not detract from the value accompanying the decision to focus continuing work on the most important obstacles whose resolution would be essential to continued cycle investment.

It is arguable that cycle R&D teams should have prioritized their work and focused on these critical path obstacles without direction from the Department of Energy. It is, however, a disappointing fact that a lot of work must be done in order to identify which obstacles are easily overcome and which are more difficult. At the same time, there could be cases for which a single step or a single component will determine whether remaining challenges should be engaged. With apologies to the Hy-CuCl team, it seems self-evident that the cycle will fail absent an effective and durable electrolyzer. Although the hydrolysis reactor and process and the crystallizer represent significant challenges for operation, especially for optimal operation, their performance in the scheme of hydrogen production is irrelevant if the electrolyzer is not effective. It could also be said of the volatile metal oxides that once it became apparent that recombination would prevent metal recovery for recycling, all other work should have been stopped or at least reduced in favor of resolution of this critical issue.

Obviously, some preliminary work must be done to identify where off-ramps are, but project planning to identify and prosecute off-ramps should be emphasized for projects that are meant to develop and deploy technology. Instead of identifying all cycle elements and planning the R&D program to address each, the planning should focus on centrally critical elements of the cycle for focused attention. Experience has identified the electrolyzer as centrally critical for hybrid cycles, recombination is centrally critical for volatile metal oxides, and durability and chemical stability is centrally critical for non-volatile metal oxides. A legitimate question is whether the

foregoing could have been projected without all the work that preceded the evaluation. The answer is not clear to this author, but it is clear that project planning has not emphasized identification and prosecution of off-ramp issues. Instead, researchers were encouraged from the outset to project overall cycle performance within the framework of stated performance targets. That emphasis would encourage teams to do as much as they could do easily and make assumptions about those parts that are, or were, too difficult to complete for performance projections. So the easiest problems would be addressed first and the most difficult problems addressed last. The easy parts are seldom off-ramp topics.

There is no easy fix to this problem of project planning for technology development and deployment. A step forward would be to engage a set of disinterested experts to assist in project planning to help define investment priorities for each project. Expert opinion could help identify “off-ramp” issues and could help define how much progress would be needed for some technical issues to be set aside in favor of focus on unresolved obstacles. This approach would entail continuing review and planning and would require significant flexibility on the part of research teams. Continual review, re-planning and flexibility are foreign to many noncommercial research and development teams and so implementation of this approach would come with its own set of barriers. Nevertheless, it is this kind of effort prioritization that distinguishes development for deployment from research for the sake of knowledge gain.

5.3.2 Selection process

The breadth of technology and scientific areas reflected by STCH R&D exceeds the expertise of any single individual. Whereas the research teams do encompass the needed expertise, it is not possible to argue that their contributions in the form of review and recommendation will always be objective and without conflict. The formality of an independent review and evaluation executed by a carefully chosen body of experts is regrettable, but such an approach appears to be the best one to make decisions that affect the disposition of Federal resources. The final recommendation is that the Department of Energy establish a technical review and advisory panel of experts whose other activities are unrelated to STCH and its participants. This group would be charged with review and recommendation to the Department regarding termination, continuation or prioritization of STCH projects. Schedule for the review process would be determined by the Department as would content and form of assessments and recommendations.

Reference Materials

1. Dorner, S. and Schnurr, W. "Hydrogen production from water by reactor heat" Nucl. Sci. Abstr. **30**(1) (1974).
2. Porter, J. T. II and Russell, J. L. Jr "Production of Hydrogen from Water" General Atomics Report GA-A12889 (1974).
3. Sato, S. and Nakajima, H. "New class of thermochemical hydrogen production processes" Journal of Nuclear Science and Technology **12**(10) (1975).
4. Bamberger, C. and Richardson, D. "Hydrogen production from water by thermochemical cycles" Cryogenics **16**(4) (1976).
5. Brecher, L. E. , Spewok, S. and Warde, C. J. "The Westinghouse Sulfur Cycle for the thermochemical decomposition of water" Conf. Proc. - World Hydrogen Energy Conf. **1** (1976).
6. Cremer, H. , Steinborn, G. and Knoche, K. F. "A thermochemical process for hydrogen production" Int.J. of Hydrogen Energy **1** (1976).
7. DeGraaf, J. , Halvers, L. , Porter, J. T. II and Russell, J. L. Jr "Engineering Design of a Thermochemical Water-Splitting Cycle" Final Report General Atomics Report GA-A13726 (1976).
8. Kittle, P. A., Mahoney, D. and Schuler, J. "A low temperature, three-step water splitting process" Conf. Proc. - World Hydrogen Energy Conf., **1**(3A) (1976).
9. Ohta, T., Kamiya, N., Yamaguchi, M., Gotoh, N., Otagawa, T. and Asakura, S. "Water-splitting-system synthesized by photochemical and thermoelectric utilizations of solar energy" Conf. Proc. - World Hydrogen Energy Conf. **1**(3A), 19-30. Publisher: Univ. Miami, Coral Gables, Fla (1976).
10. Brecher, L. E. , Spewok, S. and Warde, C. J. "Westinghouse sulfur cycle for the thermochemical decomposition of water" Int. J. Hydrogen Energy **21** (1977).
11. Knoche, K. F. "Status of hydrogen production with nuclear process heat" Chem.-Ing.-Tech. **49** (1977).
12. Bamberger, C. E. "Hydrogen production from water by thermochemical cycles; a 1977 update" Cryogenics **18**(3) (1978).
13. Dafler, J. R., Foh, S. and Schreiber, J. "Assessment of thermochemical hydrogen production" Inst. Gas Technol., Chicago,IL,USA. (1978).
14. Chuang, M. C. "A study on utilizing solar energy for hydrogen production" AIChE Symp. Ser. **75**(189) (1979).
15. Farbman, G. and Fiebelmann, P. "The Westinghouse sulfur cycle hydrogen production process: program status" Hydrogen Energy Syst., **5** 2485-2504 (1979).

16. Fiebelmann, P., Flamm, J., Lalonde, D., Langenkamp, H., Schuetz, G. and Van Velzen, D. "Development, design and operation of a continuous laboratory-scale plant for hydrogen production by the Mark-13 cycle" Hydrogen Energy Syst., **2** 649-665 (1979).
17. Liu, F., Kondo, W., Kumagai, T., Oosawa, Y., Takemori, Y. and Mizuta, S. "The magnesium-iodine cycle for the thermochemical decomposition of water" Hydrogen Energy Syst., **2** (1979).
18. Boltersdorf, D., Gehrmann, J., Junginger, R. and Struck, B. D. "Anodic oxidation of sulfur dioxide in the sulfuric acid hybrid cycle" Int. J. Hydrogen Energy **55** (1980).
19. Carty, R. H. and Conger, W. L. "Heat penalty and economic analysis of the hybrid sulfuric acid process" Int. J. of Hydrogen Energy **51** (1980).
20. Ducaroir, M., Tmar, M. and Bernard, C. "Possibilities of solar energy storage using sulfates" Revue de Physique Appliquee **15**(3) (1980).
21. Pangborn, J. "Experimental Work on a CdO based Solar Cycle for Water Splitting", Proceed. of the STTFUA, **28**(11) (1980).
22. Williams, L.O. "Hydrogen Power: An Introduction to Hydrogen Energy and Its Applications", Pergamon Press, (1980).
23. Bilgen, E. and Bilgen, C. "Solar Synthetic Fuel Production", Int. J. Hydrogen Energy, **6**(4) (1981).
24. Remick, R., Schreiber, J. and Foh, S. "A cadmium-cadmium hydroxide thermochemical water-splitting cycle" Advances in Hydrogen Energy **2** (1981).
25. Knoche, K. F. "High-temperature process heat for thermochemical splitting of water" VGB Kraftwerkstech. **62**(12) (1982).
26. Langenkamp, H. and Van Velzen, D. "Status report on the operation of the bench-scale plant for hydrogen production by the Mark-13 process" Int. J. Hydrogen Energy **7**(8) (1982).
27. Bremen, J., Hartmann, H. and Von Wolfersdorff, W. "Separation of sulfur dioxide and oxygen by absorption" Int. J. Hydrogen Energy **8**(2) (1983).
28. Pierre, J. and Yannopoulos, L. N. "Hydrogen production process: High temperature-stable catalysts for the conversion of SO_3 to SO_2 " Int. J. Hydrogen Energy **9**(5) (1984).
29. Ambriz, J.J. "Hydrogen Production from Cd/CdO Thermochemical Cycle Using a Solar Furnace" H_2 Produced from Renewable Energy (2nd Int Symp) (1985).
30. Bilgen, E. and Joels, R. K. "An assessment of solar hydrogen production using the Mark 13 hybrid process" Int. J. Hydrogen Energy **10**(3) (1985).
31. Upadhyay "Thermodynamic Investigation of a Thermochemical Cycle of Fe-Cl Family for the Production of H_2 ", **1** (1985).
32. Hakajima, H., Ikezoe, Y., Onuki, K., Sato, S. and Shimizu, S. "Studies on the Ni-I-S Process for Hydrogen Production" Int. J. Hydrogen Energy **11**(9) (1986).
33. Kumagi, T. and Mizuta, S. "Continuous Flow Demonstration of the Mg-S-I Cycle for Thermochemical Hydrogen Production" Chem. Lett. (1986).
34. Liao, X. "A new hybrid thermochemical cycle for production of hydrogen from water" Scientia Sinica, Series B: Chemical, Biological, Agricultural, Medical & Earth Sciences **29**(7) (1986).
35. Engels, H., Funk, J., Hesselmann, K. and Knoche, K. F. "Thermochemical Hydrogen Production" Int. J. Hydrogen Energy **12**(5) (1987).

36. Pretzel, C.W. "The Developmental Status of Solar Thermochemical Hydrogen Production", SAND86-8056, (1987).

37. De Bruin, D. and Onstott, E. I. "Thermochemical Hydrogen Production with the Sulfur Dioxide-Iodine Cycle by Utilization of Diprasedymium dioxygenmonosulfate as a Recycle Reagent" *Int. J. Hydrogen Energy* **13**(1) (1988).

38. Hayashi, H., Mitate, T. and Takehara, Z. "Hybrid process for hydrogen production by the use of hydrobromic acid electrolysis in lithium bromide-potassium bromide melts" *Int. J. Hydrogen Energy* **12**(5) (1988).

39. Ikenoya, A., Kumagai, N., Liao, X., Tanno, K. and Yashiro, H. "Studies on the KNO₃-I₂ Hybrid Cycle for Hydrogen Production" *Int. J. Hydrogen Energy* **13**(5) (1988).

40. Knoche, K. F. and Roth, M. "Thermochemical Water Splitting Through Direct HI- Decomposition from H₂O/HI/I₂" *Int. J. Hydrogen Energy* **14** (1989).

41. Yalcin, S. "A Review of Nuclear Hydrogen Production" *Int. J. Hydrogen Energy* **14** (1989).

42. Kumagi, T. and Mizuta, S. "Continuous Flow System Demonstration and Evaluation of Thermal Efficiency for the Magnesium-Sulfur-Iodine Thermochemical Water-Splitting Cycle" *Ind. Eng. Chem. Res.* **29** (1990).

43. Wendt, H. "Electrochemical Hydrogen Technologies", Elsevier, (1990).

44. Lundberg, M. "Model calculations on some feasible two-step water splitting processes" *Int. J. Hydrogen Energy* **18** (1993).

45. Berndhauser, C. and Knoche, K. F. " Experimental Investigations of Thermal HI Decomposition from H₂O-HI-I₂ Solutions" *Int. J. Hydrogen Energy* **19** (1994).

46. Tamaura, Y. "Production of Solar Hydrogen by a Novel, 2-Step, Water Splitting thermochemical Cycle", *Energy*, **20**(4) (1995).

47. Tamaura, Y., Yoshida, S., Kawabe, M., Hosokawa, Y. and Tsuji, M. "Conversion of Solar Energy to Chemical Energy of H₂ Gas: H₂ Production Cycle Using 2-Step Water-Splitting in the Na-Fe-O System" *Nippon Kagakkai Koen Yokoshu* **74**(1) (1998).

48. Ganz, J. , Nuesch, P. , Schelling, T. and Sturzenegger, M. "Solar hydrogen from a manganese oxide based thermochemical cycle" *Journal de Physique IV* **9** (1999).

49. Hasegawa, N. , Matsunami, J. , Nezuka, M. , Sano, T. , Tamaura, Y. , Tsuji, M. , Ueda, Y. "Solar Hydrogen Production by Using Ferrites" *Solar Energy* **65**(1) (1999).

50. Nuesch, P. and Sturzenegger, M. "Efficiency analysis for a manganese-oxide-based thermochemical cycle" *Conference Proceedings: Energy* (Oxford) **24** (1999).

51. Berman, A. and Epstein, M. "Kinetics of hydrogen production in the oxidation of liquid zinc with water vapor" *Int. J. Hydrogen Energy* **25**(10) (2000).

52. Weidenkaff, A. , Reller, A. W. , Wokaun, A. and Steinfield, A. "Thermogravimetric analysis of the ZnO/Zn water splitting cycle" *Thermochimica Acta* **359** (2000).

53. Gokon, N., Inoue, M., Hasegawa, N., Kaneko, H., Tamaura, Y., Uehara, R. and Kojima, N "Stoichiometric studies of H₂ generation reaction for H₂O/Zn/Fe₃O₄ system" *Int. J. Hydrogen Energy* **26**(9) (2001).

54. Kurata, Y., Akino, N., Sakurai, M., Onuki, K., Nakajima, H., Shimizu, S., Ioka, I., Futakawa, M., Hwang, G., Ishiyama S., Kubo, S. and Higashi, Shun'Tchi "A study on the thermochemical IS process" Nuclear Production of Hydrogen, Information Exchange Meeting, 1st,

Paris, France, Oct. 2-3, 2000 (2001), Meeting Date 2000, 129-136. Publisher: OECD Publications and Information Center, Washington, D. C (2001).

55. Gokon, N., Inoue, M., Hasegawa, N., Kaneko, H., Tamaura, Y. and Uehara, R. "XPS Analysis in Hydrogen Generation Reaction of Two-step Water Splitting Using Zn-ferrite" Kotai no Hannosei Toronkai Koen Yokoshu **13** (2002).

56. Brown LC, Besenbruch GE, Lentsch RD, Schultz KR, Funk JF and Pickard PS "High Efficiency Generation of Hydrogen Fuels Using Nuclear Power" General Atomics Report GA-A24285. Prepared under the Nuclear Energy Research Initiative Program for the US Department of Energy, Dec. (2003).

57. Pierrard, P., Goldstein, S., Borgard, J., Powers, D., Pickard, P., Brown, L., Funk, J., Schultz, K. and Besenbruch, G. "An international laboratory-scale demonstration of the sulfur-iodine thermochemical water-splitting cycle" American Institute of Chemical Engineers, [Spring National Meeting], New Orleans, LA, United States, Mar. 30-Apr. 3, (2003).

58. Kodama, T., Yamamoto, R., Kondo, Y. and Shimizu, K. "Thermochemical water-splitting by reactive ceramic materials (1) Two-step cycle by using ZrO₂-supported ferrite" Nippon Kagakkai Koen Yokoshu **83**(1) (2003).

59. Fujiwara, S., Ikenoya, K., Onuki, K., Onuki, K., Nakajima, H., Nakajima, H., Shimizu, S., Futakawa, M., Kasahara, S., Hwang, G., Choi, H., Nomura, M., Ishiyama S., Kubo, S., Kubo, S. and Higashi, S. "Application of an electrochemical membrane reactor to the thermochemical water splitting IS process for hydrogen production" Journal of Membrane Science **240** (2004).

60. M. Serban, M.A. Lewis MA, J.K. Basco, "Kinetic study for the hydrogen and oxygen production reactions in the copper-chlorine thermochemical cycle" Conference Proceedings, 2004 AIChE Spring National Meeting, pp. 2690-2698 (2004).

61. Perkins, C. and A.W. Weimer, "Likely Near Term Solar-thermal Water Splitting Technologies," Int. J. Hydrogen Energy **29** (15), 1587-1599 (2004).

62. Abanades, S., Charvin, P., Flamant, G. and Pierre Neveu "Screening of water-splitting thermochemical cycles potentially attractive for hydrogen production by concentrated solar energy" Energy, **31**(14) 2805-2822 (2006).

63. McQuillan, B., Gottfried E. Besenbruch, Lloyd C. Brown, Roger A. Rennels and Bunsen Y. Wong "Metal Sulfate Water-Splitting Thermochemical Hydrogen Production Cycles", Proceedings of the 16th World Hydrogen Energy Conference, Lyon, France, June 13-16 (2006).

64. Wong, B., Lloyd C. Brown, Gottfried E Besenbruch, Yitung Chen, Richard Diver, B. Earl, Sean H. T. Hsieh, K. Kwan, Barry W. McQuillan, C. Perkins, P. Phol, Roger Rennels, N. Siegel and Alan Weimer "Evaluation of Water-Splitting Cycles Applicable to Solar Thermal Systems", Proceedings of the 13th International Symposium on Concentrated Solar Power and Chemical Energy Technology (SolarPACES), Seville, Spain, June 20-23 (2006).

65. Francis, T., Casey S. Carney, Paul R. Lichy, Roger Rennels, and Alan W. Weimer, "The Rapid Dissociation Of Manganese Oxide To Produce Solar Hydrogen," Annual Meeting of the American Institute of Chemical Engineers, Salt Lake City, UT Nov (2007).

66. Kilbury, O., Casey S. Carney, Hans Funke and Alan W. Weimer, "Improving Sodium Recovery in the Hydrolysis Step of a Manganese-Oxide Thermochemical Cycle for Hydrogen Production," Annual Meeting of the American Institute of Chemical Engineers, Salt Lake City, UT Nov (2007).

67. Perkins, C. and A.W. Weimer, "Computational Fluid Dynamics Simulation of a Tubular Aerosol Reactor for Solar-thermal ZnO Decomposition," Journal of Solar Energy Engineering, **129**, 391-404 (2007).

68. Perkins, C., P.R. Lichty, and A.W. Weimer, "Determination of Aerosol Kinetics of Thermal ZnO Dissociation by Thermogravimetry," Chemical Engineering Science **62**, 5952-962 (2007).

69. Perkins, C., P.R. Lichty, C. Bingham, and A.W. Weimer, "Effectiveness of a Fluid-wall for Preventing Oxidation in Solar-thermal Dissociation of ZnO," AIChE Journal, **53**(7), 1830 (2007).

70. Kolb, G. J., R. Diver and N. Siegel, "Central Station Solar Hydrogen Power Plant" Journal of Solar Energy Engineering, American Society of Mechanical Engineers, May (2007).

71. Siegel, N.P., et al., "Solid particle receiver flow characterization studies", ASME Proceedings of Energy Sustainability 2007, ES2007-36118, (2007).

72. Huajun Chen, Yitung Chen, and Hsuan-Tsung Hsieh, "Computational Fluid Dynamics Modeling of Gas-Particle Flow within a Solid-Particle Solar Receiver", Journal of Solar Energy Engineering-Transactions of the ASME, **129** pp. 160-170, (2007).

73. Perkins, C., P.R. Lichty, and A.W. Weimer, "Thermal ZnO Dissociation in a Rapid Aerosol Reactor as part of a Solar Hydrogen Production Cycle," Int.J. of Hydrogen Energy, **33**(2), 499-510 (2008).

74. Funke, H.H., H. Diaz, X. Liang, C.S. Carney, and A.W. Weimer, "Hydrogen Generation by Hydrolysis of Zinc Powder Aerosol," Int. J. of Hydrogen Energy, **33**, 1127 1134 (2008).

75. Vijayarangan, B.R., Moujaes, S., Flores, M., "Particle Attrition Analysis in a High Temperature Rotating Drum," Proceedings of the Nineteenth Annual Conference On Systems Engineering, pp. 512-518 (2008).

76. Perkins, C. and A.W. Weimer, "Solar-thermal Production of Renewable Hydrogen," AIChE Journal **55**(2), 286-293(2009).

77. Haussener, S., D. Hirsch, C. Perkins, A.W. Weimer, A. Lewandowski, A. Steinfeld, "Modeling a Multitube High-temperature Solar Thermochemical Reactor for Hydrogen Production," Journal of Solar Energy Engineering, **131**, 024503 (2009).

78. M. Ferrandon, M. Lewis, D. Tatterson, A. Gross, D. Doizi, L. Croizé, V. Dauvois, J.L. Roujou, Y. Zanella, P. Carles, "Hydrogen Production by the Cu-Cl Thermochemical Cycle: Investigation of the Key Step of Hydrolyzing CuCl₂ to Cu₂OCl₂ and HCl Using A Spray Reactor, to be published in International Journal of Hydrogen Energy.

79. M. A. Lewis and J. G. Masin, P.A.O'Hare "Evaluation of alternative thermochemical cycles. Part I: The methodology" Int. J. Hydrogen Energy. **34** 4115-4124 (2009).

80. M. A. Lewis and J. G. Masin, "The evaluation of alternative thermochemical cycles – Part II: The down-selection process" Int. J. Hydrogen Energy **34**, 4125-4135 (2009).

81. M.A. Lewis, M.S. Ferrandon, D.F. Tatterson, P. Mathias, "Evaluation of alternative thermochemical cycles – Part III further development of the Cu–Cl cycle" Int. J. Hydrogen Energy **34**, 4136-4145 (2009).